MICROSTRUCTURAL AND *IN VIVO* WEAR ANALYSIS OF ALL-CERAMIC AND METAL-CERAMIC CROWNS AND THEIR ENAMEL ANTAGONISTS

By

JOSEPHINE F. ESQUIVEL-UPSHAW

A THESIS PRESENTED TO THE GRADUATE SCHOOL OF THE UNIVERSITY OF FLORIDA IN PARTIAL FULFILLMENT OF THE REQUIREMENTS FOR THE DEGREE OF MASTER OF SCIENCE

UNIVERSITY OF FLORIDA

2010

To my parents who nurtured my incessant desire to be a lifetime learner; to my mentors who helped me pursue my academic interests with zeal and encouragement; to my husband and children who persevered through the roughest of times, I am forever grateful

ACKNOWLEDGMENTS

I thank Drs. Kenneth Anusavice and Buddy Clark for their mentoring throughout my whole career in academia, Dr. Bill Rose for his assistance and friendship during this study, and Ivoclar Vivadent for their generous support of this project. I would also like to thank the faculty and staff of the Advanced Post-graduate Program in Clinical Investigation (APPCI) for steering me in the right direction. I thank Dr. Chuchai Anumana, Ben Lee and Allyson Barrett for their technical support and all the patients who persevered.

TABLE OF CONTENTS

page

LIST OF TABLES

LIST OF FIGURES

Abstract of Thesis Presented to the Graduate School
of the University of Florida in Partial Fulfillment of the
Requirements for the Degree of Master of Science

MICROSTRUCTURAL AND IN VIVO ANALYSIS OF ALL-CERAMIC ANDMETAL-CERAMIC CROWNS AND THEIR ENEMAL ANTAGONISTS

By

Josephine F. Esquivel-Upshaw

May 2010

Chair: Nabih Asal
Major: Medical Sciences – Clinical and Translational Science

Objectives: (1) To characterize the microstructure (crystal size and volume fraction of crystal and glass phases) and physical properties (fracture toughness and hardness) of a single type of a veneering ceramic for metal ceramic prostheses (IPS d.SIGN) and two different all ceramic materials (IPS Eris and IPS e.max Press); (2) To test the hypothesis that microstructural characteristics of the ceramic do not influence the wear of ceramic on the opposing enamel; (3) To test the hypothesis that bite force does not correlate with wear of either a ceramic or of an enamel antagonist.

Methods: We conducted a randomized, controlled clinical trial to analyze the wear of enamel against ceramic antagonist restorations. This single-blind pilot study involved a total of 31 patients (8 male, 23 female; age range 24-62 years) with 36 teeth that needed full coverage crowns opposing natural antagonist teeth. Thirty six (36) teeth were randomly assigned to receive either a metal-ceramic (IPS d.SIGN, Ivoclar Vivadent) or an all-ceramic crown (IPS Empress 2 with Eris or IPS e.max Press, Ivoclar Vivadent). Maximum biting force was measured for each patient using a gnathodynamometer. A single unit crown was fabricated from either one of two all-

ceramic materials or a metal-ceramic material. A vinyl polysiloxane impression was made of the maxillary and mandibular arches to record the occlusal surfaces of the cemented crowns, their antagonist teeth, and their contralateral teeth, after one week, one year, two years and three years, post cementation. Casts were produced in gypsum (GC Fujirock) and scanned using a 3D Laserscanner (Willytec, Germany). Maximum wear was calculated by superimposing the baseline one-week image with first, second and third year images and measuring the reduction in tooth height on the occlusal surface in microns.

Results: The mean maximum wear for the ceramic crowns (C) was 47.8±6.0 μm in year 1, 58.8 ± 6.4 μm in year 2 and 80.6 ± 9.0 μm in year 3. The mean maximum wear for the natural enamel antagonists (CA) was 59.4 ± 5.2 μm in year 1, 69.1 ± 7.8 μm in year 2 and 71.5 ± 7.1 μm in year 3. Teeth contralateral to the crowns (CC) exhibited a maximum wear of 42.4 ± 5.3 μm in year 1, 49.5 ± 6.5 μm in year 2 and 54.4 ± 6.5 μm in year 3. In contrast, teeth contralateral to the crown antagonists (CCA) exhibited a maximum wear of 66.9 ± 12.8 μm in year 1, 71.9 ± 14.9 μm in year 2 and 107.9 ± 23.8 μm in year 3. SAS PROC MIXED (α = 0.05) revealed no statistically significant difference in the mean maximum wear between the ceramic crowns, their natural antagonists, and their contralateral teeth; however, the contralateral crown antagonists displayed significantly greater wear compared with the other three groups ($p<0.001$). No correlations were found between bite force, fracture toughness, and hardness with the amount of wear of ceramics or their enamel antagonists.

Conclusion: These ceramics are promising as a long-term restorative material with *in vivo* wear rates within the range of normal enamel wear.

CHAPTER 1
INTRODUCTION

Crown and bridge prostheses are some of the most expensive restorative options for a dental patient receiving treatment. A single ceramic crown can cost between $800 and $3000 depending on materials, complexity of oral conditions (disease, occlusion, bone quality, tissue health), location in the dental arch, and the dentist's training and experience. Unfortunately, the increased demand for esthetics led to the introduction of ceramic products for crowns and fixed partial dentures (FPDs) well before the limitations of these products were fully explored. One of the major limitations of ceramics is their abrasiveness against natural antagonist tooth structure that leads to accelerated wear of enamel [1, 2]. The mechanism and the quantification of wear continue to challenge many dental scientists. Wear affects health in several ways, which include effects on supporting structures of the teeth, loss of vertical dimension, tooth sensitivity, esthetics and overall masticatory function [2]. Furthermore, wear can lead to dysfunctions of the temporomandibular joint and the head with symptoms ranging from headache and pain to decreased function. Unfortunately, very little is understood of the wear patterns, wear occurrence and the amount of wear for any particular individual [3]. Until recently, wear studies were conducted *in vitro* [1, 3-9] and showed no correlation with clinical occurrences in the mouth. Therefore, the mechanism of wear should be examined *in vivo* in relation to the microstructure of ceramic materials so that we can truly assess the effects of ceramics and wear on human health.

In vitro wear studies require wear instruments that measure wear in only one or two dimensions. The International Organization for Standardization (ISO) and the American Dental Association's (ADA) standard method for measuring wear is a pin-on-

disk system where a disk of enamel is placed on a flat surface and a pin is fabricated from the restorative material being investigated [10]. The disk is rotated and the amount of wear on the stylus is measured. Although the pin-on-disk is the simplest method of determining the amount of wear, this test is not representative of the masticatory environment. Teeth are not flat and do not rotate on a 360-degree plane. Furthermore, wear is only measured in the vertical direction and does not reflect the actual wear patterns in the mouth. The problem with these wear instruments is that none of the claims can be validated, as results cannot be compared with clinical wear.

The most difficult and pressing issue involving the wear testing of ceramics is the method by which wear occurs based on masticatory movements. The jaw moves in different directions aside from vertical and circular motions. Chewing patterns are very complex and can vary from individual to individual depending on the existence of joint pathology, occlusion and muscle tone. These *in vitro* studies fail to take into account clinically relevant wear patterns that more completely model the masticatory system.

To address the shortcomings of these *in vitro* studies, a 3D Laserscanner (Willytec Corp., Munich, Germany) was developed to measure wear clinically to an accuracy of $\pm$ 20 μm. The 3D Laserscanner [11-13] uses a laser beam that is projected through a special optic system onto the surface being studied. The reflection of the beam is observed at a defined angle by a high resolution CCD camera as per the principle of the light-slit microscope. After scanning, the laserscanner software allows reference-free 3-D superimposition of images and locates and quantifies the differences between the two images, thereby measuring the amount of wear. This device also allows measurement of wear in three dimensions, thereby giving a more realistic view of

the clinical occurrence of wear and the mechanism involved. To date, two *in vivo* [14, 15] wear studies have used this technology. While both studies are comprehensive, no correlation was reported between wear and the ceramic microscturcture or properties that might make ceramic more or less abrasive. The ultimate goal is to create a fracture resistant, wear-friendly ceramic that is esthetically pleasing. To accomplish this goal, we need to analyze the microstructure and physical properties of ceramics that affect wear of opposing enamel.

This clinical study allowed us to measure the amount of wear for both enamel and restorative material and investigate potential correlations with other health factors. This study will also assist us in the development of enamel-friendly or wear-friendly materials to be used in restorative dentistry. The main objectives of this study are to characterize the microstructure (crystal size, volume fraction of crystal and glass phases, and interparticle spacing) of three ceramic materials and to test the hypothesis that microstructure of ceramic does not affect the wear of opposing enamel. This study examined the following hypotheses: 1) A lower fracture toughness of glass and/or crystal phase in ceramics increases the wear damage of enamel, 2) A lower hardness in glass-ceramics reduces the wear damage of enamel, 3) Smaller sized crystals in a glass-ceramic veneer reduce the wear damage of enamel and 4) Maximum biting force does not correlate with maximum wear.

CHAPTER 2
BACKGROUND AND SIGNIFICANCE

Wear of Ceramic on Enamel

The abrasiveness of ceramic on enamel has been a cause of concern for clinicians and scientists alike. Numerous studies have shown that ceramic is one of the most abrasive restorative materials compared with amalgam, gold and composite [5, 16-22]. Other *in vitro* studies have also focused on the intrinsic nature of ceramic to determine if any factors affect enamel wear. These studies have examined physical as well as microstructural properties, which could contribute to the abrasive nature of ceramic. Unfortunately, there are no studies that have confirmed these findings clinically. Hardness and fracture toughness are the physical properties of ceramic that were assumed to affect the wear of enamel.

Hardness

Hardness is defined as the resistance to permanent deformation by an indenter. *In vitro* studies on various metals reported a direct correlation with the hardness of the metal and the amount of wear on enamel opposing the metal [23-25]. Originally, scientists believed that since ceramics are among the hardest materials [26], they were often utilized for grinding because of their abrasiveness. Thus, the same direct correlation should naturally exist between ceramic hardness and enamel wear. However, studies have shown that the correlation of hardness and wear of enamel may not apply to ceramics due to the brittleness and variability of ceramic hardness [27-29]. Unlike metals, veneering ceramics have a non-homogenous structure composed of a glassy matrix and crystals interspersed within this matrix. Since veneering ceramics may not have a homogenous structure, as exhibited by some metals, the wear rates of

these ceramics and the wear of enamel by these ceramics may be quite variable. The hardness of the ceramic structure is therefore influenced by whether the indenter is situated within the glassy matrix or on the crystalline structure. The location of the indenter is difficult to predict and both the crystalline phase and glassy matrix phase respond differently to indentation loads [26]. The glassy matrix tends to initially undergo minimal plastic deformation before fracture, hence the brittle nature of ceramics. The crystalline phase responds to indentation loads by having crystals dislocate within the glassy matrix [26], thereby registering higher hardness values. These factors make hardness values unreliable in predicting wear of these ceramics and their opposing enamel.

Fracture Toughness

Fracture toughness is a measure of the resistance of a material to crack propagation. Fracture toughness is controlled by several factors, which include heat treatment and crystal volume fraction [30]. Ceramics do not tolerate tensile stresses well because of their brittle nature. Tensile stresses are often introduced during mastication by oblique loading angles and the morphology of cusps and ridges on the teeth. Small cracks within the surface can propagate over time and cause a catastrophic failure of the ceramic restoration [31, 32]. This failure, often exhibited as microfractures in the ceramic, can result in the loss of the glassy matrix on the surface of the ceramic, leaving the harder, sharper and rougher crystals to abrade the opposing enamel surface, leading to increased wear. Compression loading, although better tolerated by ceramic, can also lead to subsurface tensile stresses, which also lead to fracture or chipping of ceramic surfaces [26, 33]. These rough surfaces lead to increased wear of opposing enamel. One of the goals of ceramic technology is to

develop ceramics with higher fracture toughness to enable increased resistance to crack propagation. Since the crack propagation may lead to either large or small fracture surfaces, the consequences can be catastrophic for both the ceramic restoration and the opposing enamel.

Because of the highly abrasive nature of ceramic restorations, several types of wear-friendly ceramics have been introduced. These ceramics include low fusing porcelains or glass-ceramics that consist mostly of the glass matrix [1, 34-37]. The rationale for producing these materials is that the lower the crystalline content, the less abrasive the material. Since the low-fusing ceramics consist mainly of a glass phase, they exhibit lower strength and fracture toughness than traditional ceramics with a higher crystal volume fraction. Interestingly, *in vitro* tests reveal that one of the low-fusing ceramics displayed one of the highest wear rates of opposing enamel [34, 37], while others are no less abrasive than conventional porcelain [1, 5, 35, 36]. The relationship between opposing enamel wear and fracture toughness of the abrading ceramics is still very unpredictable and clinical studies are needed to predict their behavior.

Fracture toughness was measured using the indentation technique developed by Chantikul et al. [38], which does not require a measurement of the critical flaw size. Instead, a flaw size is assumed from the indentation load used to induce controlled flaws. This method eliminates some of the investigator-related error from data collection, but this method is not accurate if environmentally-assisted slow crack growth occurs before fracture. Since these measurements will only be used to confirm data prior to the clinical study, this method is considered sufficient.

The strength values that were determined previously were used to determine fracture toughness using Equation 2-1,

$$K_{IC} = \eta_V^R \left(\frac{E}{H}\right)^{1/8} \left(\sigma_f P^{1/3}\right)^{3/4} \quad (2\text{-}1)$$

where η_V^R is a geometrical constant for a Vickers diamond, E is Young's modulus, H is the hardness, (calculated according Equation 2-2,

$$H = \frac{2P\sin\left(\frac{\theta}{2}\right)}{\bar{a}^2} \quad (2\text{-}2)$$

where P is the indentation load, θ is the angle between opposite diamond faces (136º), and $\bar{a}$ is the mean diagonal length of the indentation) σ_f is the fracture stress and P is the indentation load (4.9 or 9.8 N). The value of η_V^R has been estimated to be 0.59 [38].

Microstructural Analysis

The microstructure of a material can be analyzed through multiple instrumental and optical analyses. Each method yields specific information that elucidates the behavior of the microstructural system as a whole [39]. The microstructure and resulting potential material properties of a dental ceramic are determined in part by the elemental composition [40, 41]. The material fabrication and processing variables (temperature, number of heat treatments, cooling rates, surface treatment conditions, number of cooling cycles, etc.) all affect nucleation and crystallization [41]. These variables affect the mechanical properties (strength, wear, hardness, toughness, viscoelasticity, fractal dimension), the chemical properties and effects (dissolution, wear, toxicity), and the esthetic characteristics that mimic the natural appearance [42] as well as the color,

opacity, translucency and fluorescence. In a given microstructure, the crystals and their interfaces with the glass matrix of a glass-ceramic have the potential of creating additional stresses [39]. Consequently, the shape, size and crystal volume area play a significant role in the ceramic performance.

The data and properties that will be determined to describe microstructure-property relationships may include volume fraction (V_v), grain size, grain size distribution, intercrystal spacing, crystal phase stoichiometry, density, elastic modulus (E), Poisson's ratio (υ), Vicker's hardness (VHN) and porosity. These parameters contribute to flexural strength (σ), characteristic strength (σno), >63.3% probability of failure Weibull modulus (m), and fractal dimensional increment (D*). The grain size and volume fraction has been characterized in a systematic manner in this study to critically analyze their effect on clinical performance and survival. This process involves preparation of the samples through etching with different acid concentrations and times, image acquisition through optical microscopy and scanning electron microscopy, image enhancement, segmentation, image processing and evaluation [43]. For this study, we evaluated grain size and volume fraction in relation to wear of opposing enamel.

Grain Size

Grain size refers to the mean size of crystals within a given volume. Ceramic materials typically consist of a three-dimensional assembly of individual grains, made of individual crystals in different crystal lattice orientations. Because of their three-dimensional distribution and the varying sizes of the grains, measurement of precise grain sizes is difficult. Grain size can be measured by the line-fraction or area-fraction methods of ASTM E112 [44]. In the line-fraction method, the statistical grain size is calculated from the number of grains or grain boundaries intersecting a line of known

length or circle of known circumference. In the area-fraction method, the grain size is calculated from the number of grains within a known area. Grain size is typically measured by viewing planar or two-dimensional sections through the three-dimensional structure, polishing and etching the sample and eventually counting the number of grains that have been revealed in a unit area. The number of grains intercepted per unit area of the section N_A is then transformed into an average grain size using $D_A=N_A^{-1/2}$,where D_A is the average grain size per unit area and N_A is the number of grains per unit area [45]. In both methods of measurement, the grain size is affected by secondary phases, porosity, preferred orientation, exponential distribution of sizes, and the presence of non-equiaxed grains. In general, the smaller the grain size, the stronger and more dense the ceramic material. Grain size affects fracture toughness, flexural strength and Weibull modulus of the ceramic material. Grain size is affected by sintering temperatures, although the manufacturer's recommended firing schedules are also assumed to control the microstructure.

Porosity and Volume Fraction

Porosity refers to areas in which air has been incorporated. In ceramic materials, porosity can indicate areas of weakness where fracture can propagate faster and without hindrance. In general, the more porous a material, the weaker the material. For this study, the focus was on porosities located at the interface between the ceramic veneer and the core material. The pressable ceramic being used in this study theoretically has less porosity overall compared with manually condensed ceramics. However, studies have shown that the porosity tends to concentrate at the interface of the ceramic and the veneer [46, 47]. The location of the porosity at the interface, if

present, can be detrimental to the bond between the ceramic core and veneer, and possibly, the clinical success of the prosthesis.

Volume fraction refers to the concentration of a specific phase. This parameter is independent of scale, shape, and size distribution of the different phases in a ceramic. Measurement of the total volume fraction for crystalline phases can be accomplished through x-ray diffraction methods [45]. Local phase fractions can be determined from a planar sample of the material with regularly placed points on a grid. The volume fraction is calculated by counting the number of points that intersect the phase being determined and dividing this number by the total number of points on the grid, giving the volume of the phase relative to the total volume of the sample.

This method is clearly documented in ASTM E562 [48]. Procedure E562 is a point-fraction method based on the stereological principle of point fraction being equal to volume fraction, i.e., $P_p = V_v$. The content of a second-phase in ceramics, such as carbide whiskers in an oxide matrix, is usually expressed as a mass fraction. Volume fractions can be converted to mass fractions if the density of each phase is known. Image analysis can measure porosity, pore-size distribution and volume fractions of secondary phases by ASTM E1245. As with grain size, porosity and second-phase content have all been correlated with ceramic properties such as mechanical strength, hardness, toughness, dielectric constant and many others.

The wear of enamel is affected by the presence of crystals in the ceramic. Since the crystal phase is harder and more abrasive than the glass phase, the number of crystals, their morphology, and type as well as their distribution in the glass matrix, all affect their potential for wear of opposing enamel [18]. In composite restorations, crystal

fillers were reduced in size to produce a wear-friendly restorative material. The concept is that as the wear-friendly matrix wears the sharper harder crystals are exposed, thereby creating a rough surface with asperities, which tended to abrade the opposing enamel. As the crystals are reduced in size, the polishability of the composite improves as well as the abrasiveness [49]. However, *in vitro* analysis revealed that ceramic may behave differently. As the glass matrix either dissolves or chips away, exposing crystals as well as a rougher surface, the larger crystals tend to be dislodged more easily as opposed to the smaller crystals that remain lodged in the glass matrix [50]. The surface with the intact smaller crystals could potentially be more abrasive to enamel than the surface with the remaining glass matrix. Since crystals also have higher hardness values, we can assume that a higher volume fraction of the crystal phase would translate into greater wear of enamel. However, other factors come into play such as the types of crystals and their morphology. Studies have shown that a glass-ceramic with 45-50% volume fraction of crystals exhibits wear of enamel that is comparable to that caused by a gold alloy [18, 19]. Most of the effects of grain size and volume fraction of crystals on the wear of opposing enamel are based on *in vitro* studies. As mentioned earlier, little or no success has been achieved in attempts to correlate these findings with clinical results.

Image Analysis

The continuing development of computer image analysis programs has facilitated the ability to distinguish features on and within three-dimensional areas using a two-dimensional image incorporating the principles of stereology. The accuracy of these program analyses relies upon the quality of the image, as well as the visual discretion of the operator.

Selected material features such as crystals, pores, and fracture features may be isolated, examined, measured, and quantified based on representative fixed area samples. This process contributes to a better understanding of the material applications and effects. Several studies have confirmed the practicality and reliability of these image analysis programs [51-53].

In this clinical research study, three ceramics were prepared and the microstructure analyzed by SEM. Resulting representative images were used in an image analysis program (Image J, NIH, Public Domain) to quantify the volume fraction of crystals.

Threshold adjustments of 8-bit images and area designations will be used to define ("mask") specific, visible, material characteristics. The "set measurements" menu has 20 possibilities for quantitative analysis. For purposes of this study, the quantitative analysis will include the area of distribution, individual crystal particle size by area, width, height and median size, and the volume fraction percentage of the selected crystals.

CHAPTER 3
MATERIALS AND METHODS

Study Design

A randomized, controlled clinical trial was conducted to analyze the wear of enamel against ceramic antagonist restorations. This single-blind pilot study involved a total of 31 patients with 36 teeth that needed full coverage crowns opposing natural antagonist teeth.

Study Population

Subjects were recruited through broadcast e-mail and flyer advertisements. Subjects were selected based on the following criteria:

- Subjects were over 18 years of age with good overall health. No contraindications to dental treatment were present.
- Subjects were in good overall good dental health with no active tooth decay (caries) present and no periodontal disease. Periodontal pocket depths on all remaining teeth were not greater than 4 mm.
- Subjects had no existing temporomandibular disorder, (e.g. clicking, popping, pain on opening) or parafunctional habits (e.g. bruxism, clenching).
- Subjects needed a crown on either a second premolar, first molar or second molar on any arch. Abutment teeth were restorable and had a crown root ratio of at least 1:1. Abutment teeth had a full complement of opposing non-restored or minimally restored natural teeth. Minimally restored means nothing beyond a Class II amalgam restoration. Opposing arch did not have a full coverage restoration or a partial denture. Contralateral tooth was present.
- Subjects exhibited good oral hygiene and compliance with oral hygiene instructions as determined by the amount of plaque present in teeth.
- Subjects had a normal flow of saliva. Subjects with any medical pathologies limiting salivary volume or chronic intake of medications that minimized flow of saliva were excluded from the study.
- Subjects were willing to pay $200 for the laboratory cost of the crown and were compliant with yearly appointments.

Study Intervention

Thirty-six (36) teeth, on 31 enrolled subjects (no patient was allowed to have more than 2 study crowns), that needed full coverage crowns were randomly assigned to receive either a metal-ceramic (IPS d.SIGN, Ivoclar Vivadent) or an all-ceramic crown (IPS Empress 2 with IPS Eris veneer ceramic or IPS e.max Press, Ivoclar Vivadent). A random number table was formulated to facilitate assignment of teeth. As each patient progressed in treatment, the random number table was used to determine what type of crown material they would receive. Patients were treated at the University of Texas Health Science Center at San Antonio (UTHSCSA) Dental School between 2002 and 2007. The UTHSCSA Institutional Review Board approved the research protocol for treating human subjects. All subjects were required to sign an informed consent form prior to initiating the study. The following baseline data were collected:

- General medical history and physical examination
- Primary casts made with vinylpolysiloxane impression material
- Bite force measurement in newtons using a gnathodynamometer
- Periodontal pocket depths of abutment teeth
- Periapical radiographs of abutment teeth

Two investigators prepared all the teeth to receive crowns. Integrity (Dentsply, USA) provisional material was used to fabricate provisionals. Vinylpolysiloxane impression material (Affinis, Coltene Whaledent) was used for final impressions. Master casts were mounted in centric relation.

A single unit crown was fabricated from either one of two all-ceramic materials or a metal-ceramic material. Occlusal surface thickness of the finished crowns was measured at baseline. Adjustments to the crown were made with a high-speed handpiece and a fine diamond bur. Prior to cementation, all adjusted surfaces were

polished or glazed. All crowns were cemented with a dual-cure resin cement (Variolink II, Ivoclar Vivadent).

A baseline examination was performed one week after cementation to ensure that the patient was comfortable with the crown and no further adjustments were needed. When no further adjustments were necessary, a vinylpolysiloxane impression was made of the maxillary and mandibular arches to record the occlusal surfaces of the cemented crown and its antagonist tooth. The post-cementation casts were poured with a white gypsum material (GC Fujirock) to enable optimal scanned image contrast. A 3D Laserscanner (Willytec, Germany) was used to scan along the x, y and z axes of the casts.

The subjects were asked to return yearly after crown cementation for the next three years. Vinylpolysiloxane impressions were made of maxillary and mandibular arches and poured with Type IV stone at the six-month period. Gypsum casts of the antagonist teeth and the crowns were scanned using the 3D Laserscanner. The baseline image was superimposed with the one, two and three year images and the amount of wear in three dimensions was calculated. Wear was quantified as maximum wear referring to loss in height and maximum volume wear referring to volumetric loss of tooth structure. Teeth with fabricated ceramic crowns were labeled as C, the crown's natural enamel antagonist as CA, the tooth contralateral to the crown as CC, and the natural tooth opposing the contralateral tooth as CCA. A standard deviation greater than 25% in the scans was considered unacceptable. Casts were either re-scanned to obtain a lower standard deviation or discarded. This procedure was repeated every year for the next two years. An SEM analysis of representative wear areas (defined as

wear exceeding 100 μm for the first year) for both the crown and enamel antagonist were made to visualize wear patterns.

Analysis of Physical Properties and Microstructure of Ceramic Materials

Three ceramic materials were used for this study. First, IPS e.max Press (Ivoclar Vivadent) is a core ceramic used to support posterior crowns as well as bridges in areas of greater masticatory load. The microstructure of IPS e.max Press consists of $Li_2Si_2O_5$ lithia disilicate crystals (approximately 70%), which are embedded in a glassy matrix [46, 54, 55]. Lithia disilicate, the main crystal phase, consists of needle-like crystals measuring 3 to 6 μm in length. The flexural strength reported by the manufacturers for this core material ranges from 300 to 460 MPa depending on the test method. The fracture toughness ranges from 2.5 to 3.0 $MPa \bullet m^{1/2}$. Second, IPS Eris is a veneering porcelain designed for all ceramic core materials [56]. This ceramic is primarily used to veneer IPS Empress 2 and consists mainly of a glass matrix. IPS Eris consists of fluorapatite crystals that are widely spaced and are embedded in a glass matrix. The flexural strength for IPS Eris varies between 100 and125 MPa and fracture toughness ranges from 0.5 to 0.8 $MPa \bullet m^{1/2}$. Lastly, IPS d.SIGN glass-ceramic is used for veneering metal crowns and bridges and is composed of phases containing calcium phosphate. These phases are predominantly needle-like fluorapatite, which are provided in two uniform sizes [57]. The flexural strength and fracture toughness for IPS d.SIGN are very similar to those of IPS Eris, which are typical veneering ceramics.

Sample Preparation for Physical Properties of Ceramic Materials

Monolithic specimens of the veneer porcelain for PFM (IPS d.SIGN), the veneer porcelain for all ceramic crowns (IPS Eris) and the ceramic core (IPS e.Max Press) were subjected to *in vitro* analyses to confirm their physical properties and

microstructure and to determine any correlation with the clinical results of wear. The metal-ceramic veneer porcelain served as the control group.

Fracture Toughness

We conducted separate fracture toughness testing for this study to obtain values independent from those reported by the manufacturer. As mentioned earlier, the fracture toughness was measured using the indentation technique developed by Chantikul et al. [38], which does not require a measurement of the critical flaw size.

Three bars of each ceramic material measuring 5 mm x 5 mm x 25 mm were fired according to manufacturer's instructions and polished. Indentation cracks were induced at the center of polished specimens using a Vickers indenter at a load of 9.8 N. This indent load was selected such that the cracks were formed at the tip of the Vickers indenter without excessive cracking or chipping. Crack lengths were approximately 2-3 times longer than the size of the diamond indenter. Specimens were subjected to four-point flexure with a 20.0 mm lower span and a 6.7 mm upper span using an Instron universal testing machine (Model 5500-R) at a crosshead speed of 0.5 mm/min until failure occurred. Failure loads for the bar specimens were obtained, and the flexural failure stresses (σ_f) were calculated using Equation 3-1,

$$\sigma_f = \frac{3Px}{wt^2} \qquad (3\text{-}1)$$

where P is the failure load, x is the distance between the inner and outer supports, w is the specimen width and t is the specimen thickness.

Hardness

Hardness is defined as a resistance to indentation. A microhardness tester (Model MO Tukon Microhardness Tester, Wilson Instruments Inc., Binghamton, NY) with a

Vickers diamond was used to measure the hardness of one specimen from each group of ceramic at three different areas. Hardness specimens were finished using a metal-bonded diamond abrasive disk. The surface to be indented was polished to a 1 μm finish using an alumina slurry. The specimens were indented at four locations under loads of 4.9 N (IPS d.SIGN and IPS Eris) and 9.81 N (IPS e.Max Press). The dimensions of the indentation diagonals were measured using an optical microscope with a filar eyepiece. The hardness values were calculated according to Equation 2-2.

Elastic Modulus

Elastic modulus was calculated, using three specimens each of the two veneer ceramics and the core porcelain, from the density and the velocity of sound through the material. The velocity of sound was measured using an ultrasonic pulse apparatus (Ultima 5100, Nuson Inc., Boalsburg, PA). Shear and longitudinal waves were generated using 5 MHz piezoelectric transducers (SC25-5 and WC25-5, Ultran Laboratories, Inc., Boalsburg, PA). The transducers were coupled to the specimens using honey and glycerin for shear and longitudinal waves, respectively. The electronic delay in the pulse apparatus was subtracted from the time-of-flight before calculating the velocity of sound. Poisson's ratios were calculated using Expression 3-2,

$$\nu = \frac{1 - 2\left(\frac{v_S}{v_L}\right)^2}{2 - 2\left(\frac{v_S}{v_L}\right)^2} \qquad (3\text{-}2)$$

where vS is the shear velocity and vL is the longitudinal velocity. Young's modulus was calculated using Expression 3-3,

$$E = \frac{\rho v_L^2 (1+\nu)(1-2\nu)}{1-\nu} \qquad (3\text{-}3)$$

where ρ is the density.

Sample Preparation for Microstructural Analysis

Three discs of each ceramic material were made from a mold that was16 mm in diameter and 1.5 mm in height. Each disc was fired according to manufacturer's instructions (refer to Appendix 1 for ceramic firing schedules) and fired twice to simulate *in vivo* crown fabrication. Each disc was polished to a 1 μm polish and etched with freshly made 3% hydrofluoric acid for 10, 12 and 15 seconds.

Optical microscopy: All the discs were examined under optical microscopy at 40x magnification using an optical microscope (Omni Met Modular Imaging System, Buehler, Lake Bluff, IL, USA). Different microstructural characteristics were noted for comparison with scanning electron microscopy images and to determine sites for further examination at higher magnifications.

Scanning electron microscopy: All the discs were prepared with a gold coating for viewing under the scanning electron microscope (SEM). Two sites for each ceramic material for each etching time were examined using the SEM to determine specific characteristics noted during the optical microscope evaluation. A semi-quantitative analysis of the elements within the ceramic was made through energy dispersive spectrometry (EDS).

Image analysis: SEM images were analyzed using the Image J Image Processing and Analysis Program (Image J) (National Institutes of Health website: http://rsb.info.nih.gov/ij/index.html). This program allowed us to determine volume fraction as well as crystal size through a series of masking procedures that enabled us to isolate specific crystals. Image J can display, edit, analyze, process, save, and print

8-bit, 16-bit and 32-bit images. The program can read many image formats including TIFF, PNG, GIF, JPEG, BMP, DICOM, FITS, as well as raw formats.

Statistical Analysis

The amount of wear in microns was determined along the x, y and z axes. An initial examination of the data was performed to determine whether a standard statistical model could be used. SAS PROC MIXED was deemed to be the most suitable tool for data analysis. We also considered the fracture toughness, hardness, and biting force as covariates in the model. Due to its large variance, CCA was compared with C, CA, and CC as pairs under the unequal variance assumption. Any presence of cracks or fractures in the crowns was recorded.

CHAPTER 4
RESULTS

Physical Properties of Ceramic

We obtained mean values for fracture toughness, elastic modulus and hardness for all three ceramics used in this study. Fracture toughness ranged from 1.04 MPa•m ^{½} for IPS d.SIGN veneering ceramic, and 0.74 MPa•m ^{½} for IPS Eris veneering ceramic to 2.35 MPa•m ^{½} for IPS e.Max Press core ceramic. Elastic modulus values were 69 GPa for IPS d.SIGN, 65 GPa for IPS Eris and 104 GPa for IPS e.Max Press. Hardness values were 5.67 GPa for IPS d.SIGN, 5.50 GPa for IPS Eris and 5.65 GPa for IPS e.Max Press (Table 4-1).

Microstructural Analysis of Ceramic

All three ceramic materials used in the study were subjected to microstructural analysis. The two veneering ceramics, IPS d.SIGN and IPS Eris, and one core ceramic, IPS e.Max Press, were formed into discs, fired twice according to manufacturer's instructions, etched, and examined by optical and scanning electron microscopy. Semi-quantitative analysis was performed during scanning electron microscopy to determine the approximate percentage or distribution of elements within the material (Table 4-2). All three ceramic materials showed a predominance of silica followed by potassium. Silicon is the most predominant element in IPS e.Max Press core with some potassium and zinc. The two veneers, IPS Eris and IPS d.SIGN demonstrate approximately 50% silicon content with the remaining bulk distributed between potassium and aluminum. Other trace elements include calcium, sodium, zinc, zirconia, phosphorus and cerium.

IPS d.SIGN

As mentioned earlier, IPS d.SIGN is used as a veneering ceramic for metal substructures. IPS d.SIGN is composed of fluorapatite ($Ca_5(PO_4)_3F$) and leucite ($KAlSi_2O_6$) crystals embedded in a glass ceramic phase. Energy dispersive spectrometry reveals that IPS d.SIGN is composed of 52.1% Si, 16.0% K, 11.9% Al, 3.7% Zn, 3.2% Zr, 2.7% Ba, 2.4% Ca and 2.7% Ce (Table 4-2, Figure 4-1). Trace elements of titanium and phosphorus were also noted. Optical microscopy is unremarkable with a dispersion of possible crystals and pores throughout the specimen (Figure 4-2). The specimens were etched for 10, 12 and 15 seconds. The 12-second etching time showed the most characterization on the surface. SEM analysis of IPS d.SIGN revealed islands of leucite crystals embedded in a glassy phase and a dispersion of needle-like fluorapatite crystals. The fluorapatite crystals were most apparent in the samples of IPS d.SIGN that received 15 seconds of etching with 3% hydrofluoric acid (Figure 4-3). Note that the fluorapatite crystals were most apparent in the backscatter mode of the SEM. Also, note the microcracking of the sample, which could represent possible over-etching of the sample for 15 seconds.

The Image J analysis program yielded the volume fraction of crystals and crystal size. Through a masking process, different crystal phases were isolated to enable the program to measure volume fraction as well as crystal size (Figure 4-4). Using a representative image of the ceramic, the Image J program was able, through a series of contrasts, to mask different areas to highlight materials of interest. The program computed the volume percent of crystals over a specified area within the ceramic. This process resulted in a mean crystal volume fraction (Vv) of 0.6 for fluorapatite over an area of 15.92 μm^2 (derived from Figure 4-4d) and 10.8 for leucite over an area of 285.98

μm^2 (Figure 4-4b). Crystal or grain size analysis was more difficult because of the inhomogeneity of the material. As seen in the SEM images (Figure 4-3), IPS d.SIGN has agglomerations of leucite crystals, which vary in size, along with scattered flourapatite crystals with different orientations (captured in cross-section and lengthwise). These agglomerations were difficult to differentiate from single crystals. Thus, the Image J program analysis a range of crystal sizes from very high to very low. The average value for grain size for fluorapatite crystals is 0.034 ± 0.030 μm^2 (median of $0.027 \mu m^2$) with a range of 0.014 - 0.27 μm^2. The average crystal size of leucite is 76.1 ± 90.0 μm^2 (median 44 μm^2) with a range of 10 - 516 μm^2. As stated earlier, a precise value of crystal size is impractical because of crystal agglomerations and variations in orientations. This challenge is evidenced by the wide range, as well as the high standard deviations, of the grain size.

IPS Eris

IPS Eris is another veneering ceramic designed to veneer ceramic cores. This veneering ceramic has a high crystalline content and was designed to bond with the Empress 2 system. EDS revealed that IPS Eris is composed of 46% silicon, 23% potassium, 15% aluminum, 5% zirconium, 2% titanium, zinc and cerium. Trace elements of sodium and phosphorus were also noted (Table 4-1, Figure 4-5). Optical microscopy revealed porosities as well as surface scratches. There were some areas that exhibited geometric shapes, which could be an indication of preferential etching (Figure 4-6). Separate EDS analyses were performed inside and outside of the geometric areas to determine if any differences existed in content (Figure 4-5). A presence of aluminum was observed outside of the geometric area, which could

account for the resistance to acid etching. SEM analysis of an IPS Eris sample etched for 12 seconds showed fluorapatite crystals that are uniformly dispersed throughout the glass matrix (Figure 4-7). Although EDS did not show the presence of fluoride, which fails to confirm the presence of fluorapatite, these images represent areas where the fluorapatite may have been etched away. Note the geometric shape evident at 2K magnification in Figure 4-7. This occurrence may have been caused by the preferential etching of some areas of the sample, where the etching occurred primarily along the geometric shape. Further magnification of the sample revealed fluorapatite crystal locations (Figure 4-8). The fluorapatite crystals appeared to be distributed uniformly within the glass matrix. In the secondary mode, the fluorapatite crystals appeared to have been etched away by the acid. The backscatter mode revealed reflections of where the fluorapatite crystals used to be in relation to one another and the glassy matrix.

The volume fractions of the apatite crystals were derived through the same masking technique employed by the Image J analysis program. Although the fluoraptite crystals were not demonstrated as being present in the EDS analysis through the absence of fluoride, we believe that these images represent their locations. The Vv for apatite crystals is 35.1% over an area of 37.84 μm^2 (Figure 4-9). Crystal size determination was also a challenge with IPS Eris due to the overlapping of the fluorapatite crystals. A drawing tool was used in the program to outline representative crystals to obtain a reasonable value for grain size. The average grain size for flouorapatite crystals is 0.25 ± 0.16 μm^2 (median 0.20 μm^2) and a range of 0.06 – 0.56 μm^2.

IPS e.Max Press

IPS e.Max Press is a core ceramic used primarily as a ceramic substructure in single crowns or in up to three-unit fixed partial dentures. This core ceramic consists of lithia disilicate crystals embedded in a glassy matrix. The EDS analysis of the elemental content of IPS e.Max Press was 76% silicon, 9% potassium, 6% zinc, 4% cerium, 2% phosphorus and aluminum, and trace elements of sodium and zirconium (Table 4-1, Figure 4-10). Optical microscopy was unable to reveal sufficient microstructural detail. There appeared to be lithia disilicate crystals as well as porosities scattered uniformly throughout the structure (Figure 4-11). The optical images were insensitive to etching times. SEM analysis of an IPS e.Max Press sample etched for 12 seconds with 3% HF acid did not reveal a very clear image. Field emission SEM (FESEM) was further conducted to reveal lithia disilicate crystals dispersed in a glass matrix (Figure 4-12). Volume fraction values for lithia disilicate crystals were 54.5, 43.3, 41.7 over an area of 490.7 μm^2. These values were derived from the same FESEM image (Figure 4-13) although the masking and the analysis were performed at three different times. These differences in values might indicate the semi-quantitative nature of the image analysis processand should be approached with caution. The same limitations were found with IPS e.Max Press in regard to grain size determination. Although the crystals seemed homogenously distributed, their boundaries were difficult to determine. We employed the same technique of using a drawing tool to demarcate the edges of the crystals to obtain reasonable grain sizes. The average grain size for lithia disilicate was 253.6 $\pm$ 248.5 μm^2 (median 233.5 μm^2) and a range of 14 – 966 μm^2.

Clinical Analysis of Wear

Thirty-one subjects were enrolled for this study and 36 teeth were randomly assigned to receive full coverage restorations. Of the 31 subjects, 8 were male and 23 were female with ages ranging from 24-62 years old. After one year, one subject with a single crown dropped out of the study. Also, one subject experienced a crown fracture after 582 days in service. The subject admitted to bruxing because of numerous stressors in her life. The subject was advised to replace the crown with a full gold crown and was dismissed from the study. As a result, 29 patients and 34 teeth were analyzed for the second year of the study.

The mean maximum wear was calculated by superimposing scanned images from first, second, and third year recalls with the baseline images (Figure 4-14). Note the wear on the buccal surface of the tooth in Figure 4-14b after one year of use in the mouth. The mean maximum wear for the ceramic crowns (C) was 47.8±6.0 μm in year 1, 58.8 ± 6.4 μm in year 2 and 80.6 ± 9.0 μm in year 3. The mean maximum wear for the natural enamel antagonists (CA) was 59.4 ± 5.2 μm in year 1, 69.1 ± 7.8 μm in year 2 and 71.5 ± 7.1 μm in year 3. Another superimposed image of enamel wear after one year is shown in Figure 4-15 with the differential image showing the most wear areas in red. In contrast, teeth contralateral to the crowns (CC) exhibited a maximum wear of 42.4 ± 5.3 μm in year 1, 49.5 ± 6.5 μm in year 2 and 54.4 ± 6.5 μm in year 3. Teeth contralateral to the crown antagonists (CCA) exhibited a maximum wear of 66.9 ± 12.8 μm in year 1, 71.9 ± 14.9 μm in year 2 and 107.9 ± 23.8 μm in year 3 (Table 4-3). Mean volume wear was also calculated in cubic microns and are highlighted in blue on the same table as maximum wear (Table 4-3).

Statistical Correlations between Materials

Three types of ceramic materials were used for this study, including IPS d.SIGN, a veneering ceramic for metal-ceramic crowns, IPS Eris, a veneering ceramic for all-ceramic crowns and IPS e.Max Press, a core ceramic. No correlation was found between the amount of wear and bite force ($p=0.15$), fracture toughness ($p=0.12$), hardness ($p=0.25$) and type of ceramic material ($p=0.09$). Analysis showed significant differences in wear between the teeth in relation to their location in the mouth ($p=0.04$) and between years ($p<0.02$) (Table 4-3). Further analysis showed that CC wore less on the average than C and C less than CA. Also, year 2 showed increased wear over year 1. When CCA was analyzed alone, the time and type of ceramic material were not significant for wear (both $p>0.25$), but biting force showed a strong effect on wear ($p<0.0001$). CCA wore slightly more than C and CA ($p=0.05$), but significantly more than CC ($p=0.0006$). Although the type of material did not reach the 0.05 statistical significance level ($p=0.09$), IPS e.max Press may prove to be a more wear resistant material due to the microstructure with densely packed crystals and a higher crystal volume fraction.

Analysis of the mean volumetric wear showed similar results except that IPS e.max Press showed a significant difference in wear resistance compared with the other two types of ceramic ($p=0.006$). No wear differences were noted in the location of the mouth ($p=0.92$), type of porcelain ($p=0.63$), annual effect ($p=0.38$), or biting force effects ($p=0.21$). However, there was a significant increase in volume from year 2 to year 3 ($p=0.005$). Note that the statistical significance cannot be solely judged by the values in the tables. Two factors, biting force and patients, are not reflected. When the patient factors are considered, the between-crown standard error is usually smaller, similar to

the reduction of variance in the paired t-test. For example, there is a reduction in mean volume for CC from year 2 to year 3 in Table 4-3. This occurrence seems counter-intuitive. The reason for the increase in volume is that several of the higher volume loss patients had been dropped. When the patient's identity is considered into the statistical analysis, this contradiction vanishes.

Image Analysis

SEM image analysis of representative wear areas were taken of crowns and enamel antagonist teeth which exceeded 100 μm of wear during the first year. The first sample is a crown on the lower left first molar made from Eris veneer with a wear rate of 158.7 μm on the buccal surface. The first set of images (Figure 4-16) shows clinical photographs of the crown one week after cementation and at the one year recall. Note the rough surface on the buccal cusps after one year of use in the mouth. Additional SEM images (Figures 4-17 to 4-20) are from 10x to 100x magnification, comparing the baseline images with the first year images and highlighting the area of wear on the buccal cusps. Note that there appear to be ridges on the 25x image (Figure 4-19) that could indicate one or more fractures on the surface of the restoration. While the wear on this crown was not the highest during the first year, the wear is significant because the patient actually complained of roughness on the surface of the crown.

The second sample is representative of enamel antagonist wear on the maxillary left first molar opposing a crown on the lower left made from Eris veneer with a wear rate of 141.3 μm. The clinical image (Figure 4-21) shows the maxillary first molar during the initial placement of the opposing crown at one year. No obvious wear can be noted clinically. SEM images range from 10x to 100x magnification (Figures 4-22 to 4-25).

These images highlight the surface roughening at the wear facets where the wear occurred. The wear rates on the crown and tooth opposing these representative samples did not show any significant wear.

Table 4-1. Fracture toughness, hardness and elastic modulus values for IPS d.SIGN and IPS Eris veneer ceramics and IPS e.Max Press ceramic

Ceramic	Fracture toughness (MPa•m ^{½})	Hardness (GPa)	Elastic modulus (GPa)
IPS d.SIGN	1.04	5.67	69
IPS Eris	0.74	5.50	65
IPS e.Max Press	2.35	5.65	104

Table 4-2. Semi quantitative analysis of elements found present in the three ceramic materials

SEM EDS	Material		
	IPS d.SIGN	IPS Eris	IPS e.max Press
Element Basis			
Na/K	5.1	0.6	0.3*
Al/K	11.9	15.3	1.9
Si/K	52.1	46.4	75.9
P/K	0.1 *	0.5*	2.2
K/K	16.0	23.2	8.8
Ca/K	2.4	4.4	-
Ti/K	0.9	1.7	-
Zn/K	3.7	1.5*	6.4
Zr/L	3.2	4.9	0.5*
Ba/L	2.7	-	-
Ce/L	1.9	1.6	4.0
Atomic Basis			
Na/K	7.0	0.9	0.5
Al/K	14.1	18.4	2.2
Si/K	59.2	53.6	84.1
P/K	0.1*	0.5*	2.2
K/K	13.1	19.2	7.0
Ca/K	1.9	3.5	-
Ti/K	0.6	1.1	-
Zn/K	1.8	0.8*	3.1
Zr/L	1.1	1.7	0.2*
Ba/L	0.6	-	-
Ce/L	0.4	0.4	0.9

Analysis conditions:
*= <2 Sigma
System Resolution = 62 eV
Quantitative method: ZAF; (d.SIGN and Eris-3 iterations); (Press Core-2 iterations)
Analyzed all elements and normalized results

Table 4-3. Mean wear for the different ceramics

	Ceramic	Crown (C)	Crown antagonist (CA)	Crown contralateral (CC)	Crown contralateral antagonist (CCA)	Overall
Year 1						
Mean maximum wear*	IPS d.SIGN	56.4 ± 14.3	55.5 ± 6.99	45.1 ± 5.55	73.4±24.2	57.2 ± 6.89
Mean volume wear**	IPS d.SIGN	0.97 ± 0.22	0.90 ± 0.10	0.97 ± 0.17	1.09 ± 0.14	0.98 ± 0.08
Mean maximum wear	IPS Eris	52.6 ± 8.99	57.7 ± 8.78	47.8 ± 17.3	36.9 ± 3.81	48.9 ± 4.78
Mean volume wear	IPS Eris	1.01± 0.25	0.92 ± 0.12	0.75 ± 0.25	0.67 ± 0.05	0.85 ± 0.09
Mean maximum wear	IPS e.max Press	36.5 ± 4.25	51.3 ± 12.2	34.1 ± 4.55	96.2 ± 30.8	52.9 ± 8.24 (37)
Mean volume wear	IPS e.max Press	0.69 ± 0.06	0.79 ± 0.12	0.71 ± 0.10	1.01 ± 0.14	0.79 ± 0.05
Mean maximum wear	Combined	47.8 ± 6.01	59.4 ± 5.2	42.4 ± 5.3	66.9 ± 12.8	
Mean volume wear	Combined	0.89 ± 0.11	0.87 ± 0.06	0.83 ± 0.10	0.93 ± 0.09	
Year 2						
Mean maximum wear	IPS d.SIGN	56.9 ± 13.3	78.9 ± 14.5	49.7 ± 5.51	85.7± 33.7	66.8 ± 8.77
Mean volume wear	IPS d.SIGN	0.87 ± 0.19	1.00 ± 0.12	1.15 ± 0.30	1.11 ± 0.24	1.03 ± 0.11
Mean maximum wear	IPS Eris	78.9 ± 9.86	58.0 ± 10.2	65.7 ± 22.2	59.2 ± 21.7	66.0 ± 7.53
Mean volume wear	IPS Eris	1.25± 0.14	0.92 ± 0.16	1.12 ± 0.50	0.86 ± 0.17	1.04 ± 0.11
Mean maximum wear	IPS e.max Press	41.1 ± 4.57	67.1 ± 14.7	35.3 ± 6.81	68.5 ± 17.6	52.8 ± 6.12
Mean volume wear	IPS e.max Press	0.74 ± 0.09	0.74 ± 0.10	0.50 ± 0.08	0.76 ± 0.10	0.70 ± 0.05
Mean maximum wear	Combined	58.8 ± 6.44	69.1 ± 7.83	49.5 ± 6.47	71.9 ± 14.9	
Mean volume wear	Combined	0.94 ± 0.10	0.90 ± 0.08	0.95 ± 0.14	0.93 ± 0.11	

Table 3-1. Continued

	Ceramic	Crown (C)	Crown antagonist (CA)	Crown contralateral (CC)	Crown contralateral antagonist (CCA)	Overall
Year 3						
Mean maximum wear	IPS d.SIGN	87.6 ± 15.9	73.7 ± 9.36	53.8 ± 7.68	108.7±41.6	81.0 ± 11.1
Mean volume wear	IPS d.SIGN	1.48 ± 0.20	1.10 ± 0.10	0.93 ± 0.15	1.44 ± 0.28	1.24 ± 0.10
Mean maximum wear	IPS Eris	95.2 ± 16.3	73.7 ± 16.0	54.6 ± 21.1	116.2 ± 43.3	87.3 ± 12.3
Mean volume wear	IPS Eris	1.31± 0.17	1.02 ± 0.20	0.67 ± 0.23	1.35 ± 0.35	1.13 ± 0.12
Mean maximum wear	IPS e.max Press	67.8 ± 11.5	66.5 ± 16.1	54.8 ± 14.5	98.1 ± 36.4	70.2 ± 9.58
Mean volume wear	IPS e.max Press	1.06 ± 0.12	0.80 ± 0.09	0.80 ± 0.22	0.81 ± 0.13	0.87 ± 0.07
Mean maximum wear	Combined	80.6 ± 9.04	71.5 ± 7.10	54.4 ± 6.52	107.9 ± 23.8	
Mean volume wear	Combined	1.32 ± 0.13	0.99 ± 0.07	0.84 ± 0.11	1.26 ± 0.17	

Year 1, Year 2 and Year 3 show progressive wear.
*Mean maximum wear shown in microns
**Mean volume wear shown in cubic microns

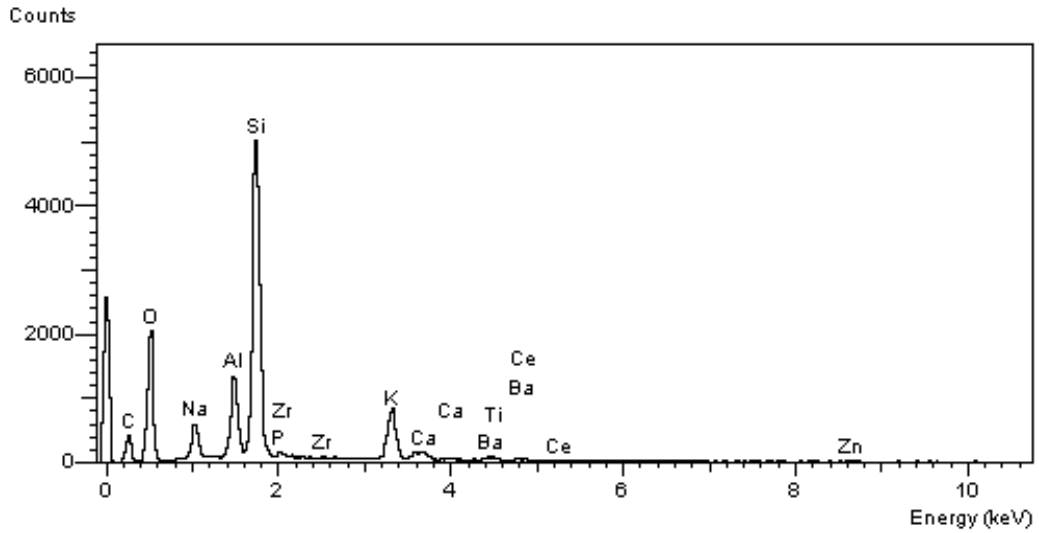

Figure 4-1. EDS spectrum depicting semi-quantitative analysis of IPS d.SIGN sample etched for 15 seconds.

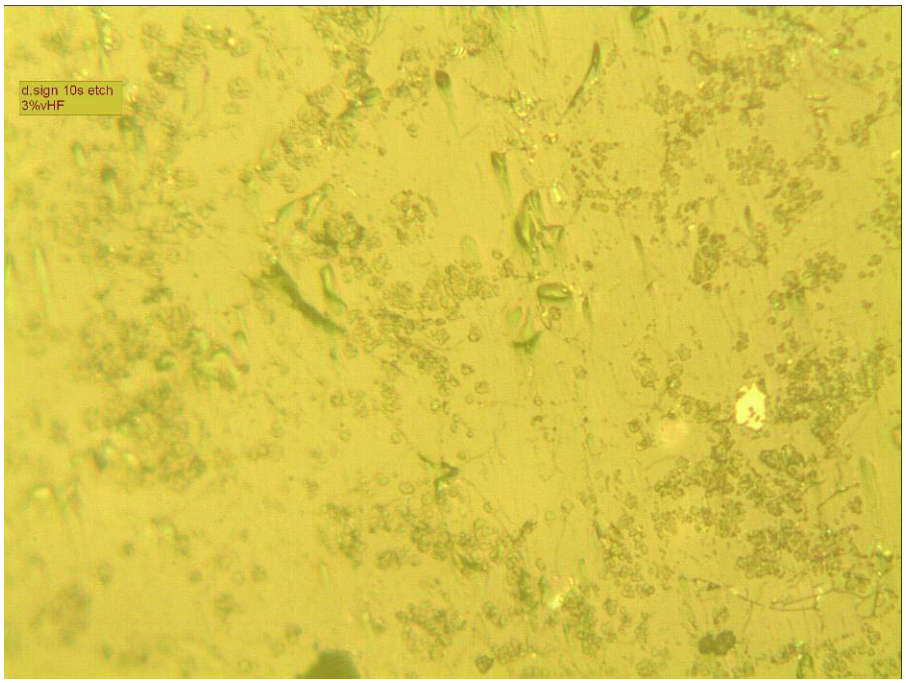

A

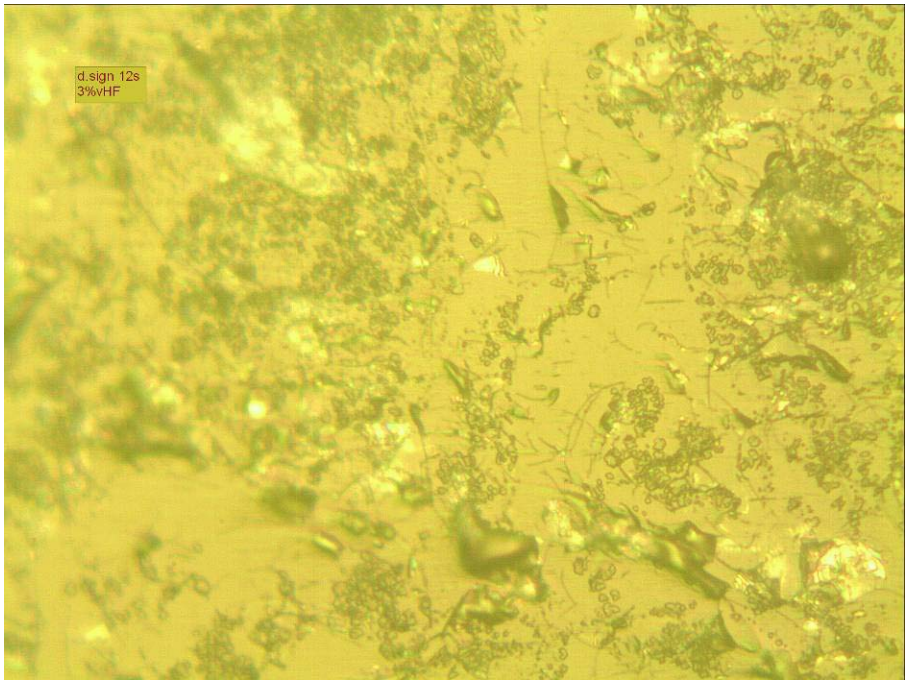

B

Figure 4-2. Optical microscopy of d.SIGN veneer ceramic showing dispersion of leucite crystals with some scattered pores. A) d.SIGN ceramic etched at 10 seconds. B) d.SIGN ceramic etched for 12 seconds. C) d.SIGN ceramic etched for 15 seconds.

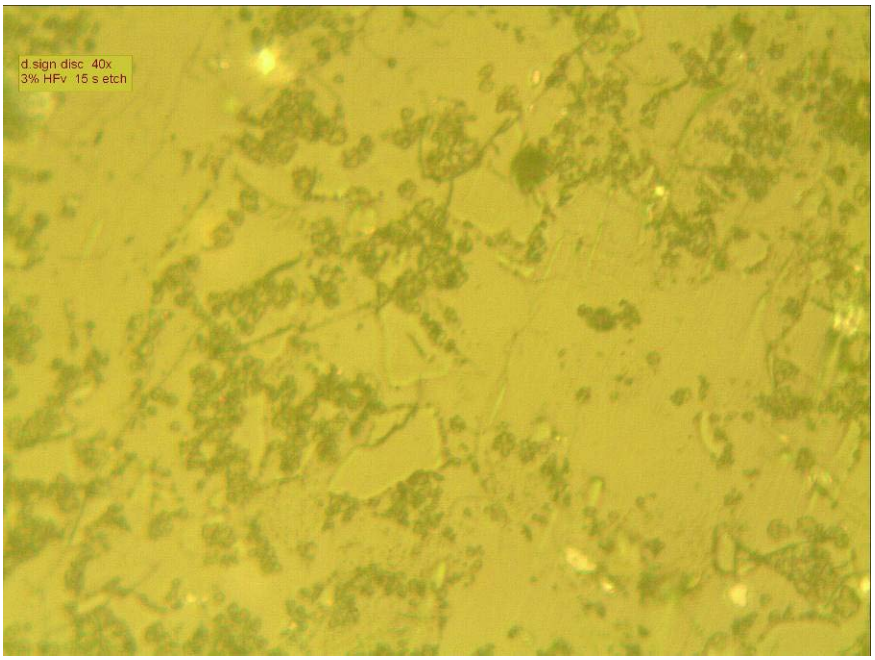

C

Figure 4-2. Continued

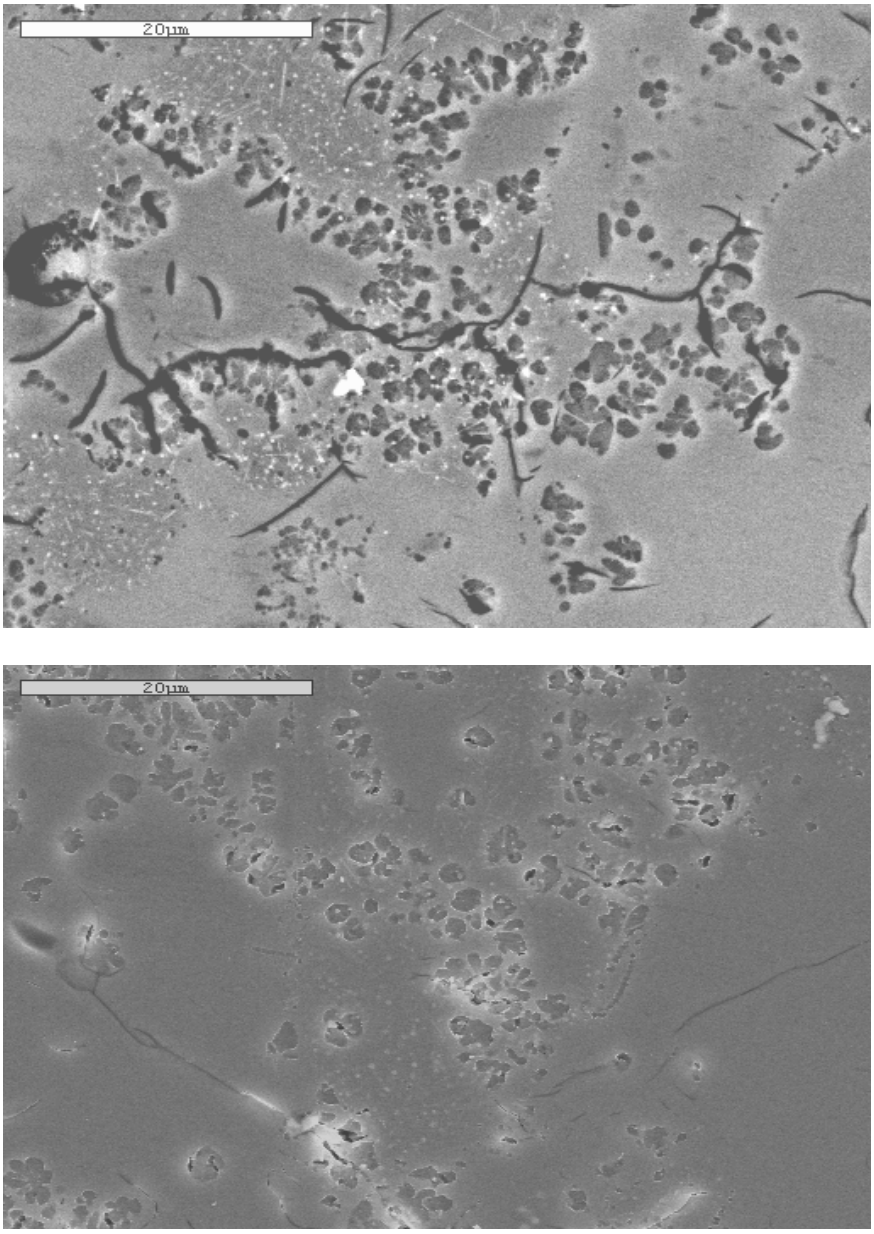

Figure 4-3. SEM images at 2K magnification. A) backscattered electron mode. B) secondary electronmode of IPS d.SIGN specimen etched for 15 secs with 3% HF acid. Fluorapatite crystals are clearly seen in the backscatter mode as white dots and needle-like structures. C) SEM analysis at 5K magnification, backscatter mode, of the microstructure of IPS d.SIGN with sample etched for 15 seconds with 3% HF acid. Note needle-like projections depicting fluorapatite crystals (blue arrow). Circular projections represent the same crystals at cross section (orange arrow). Leucite crystals are depicted as clusters throughout the glassy matrix (yellow arrow). D) SEM of same specimen in secondary mode. Note that fluorapatite crystals are not very distinct in this mode even though it is of the same sample area as the SEM image in 4-3A.

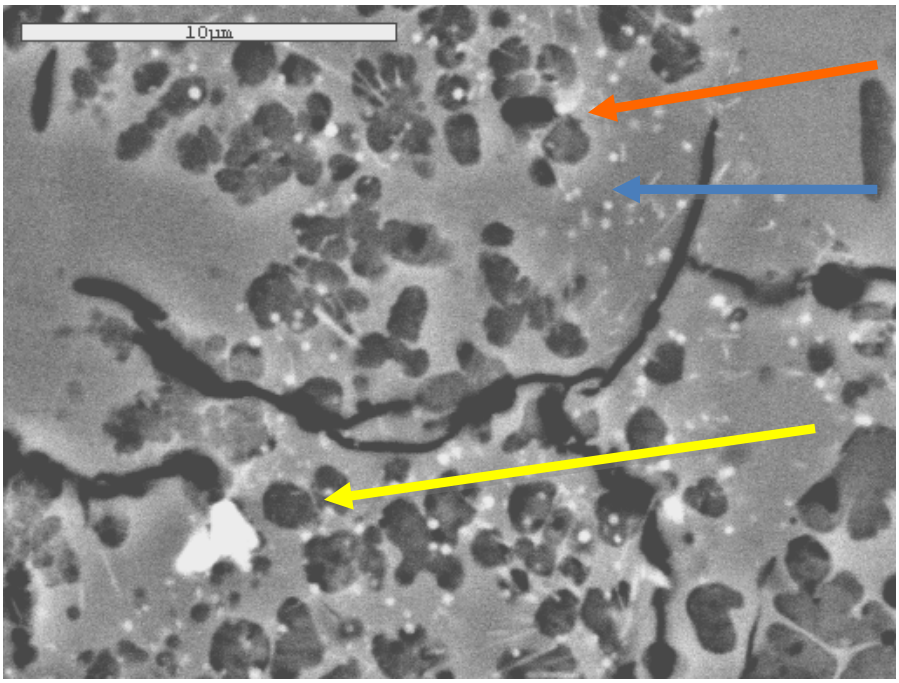

C

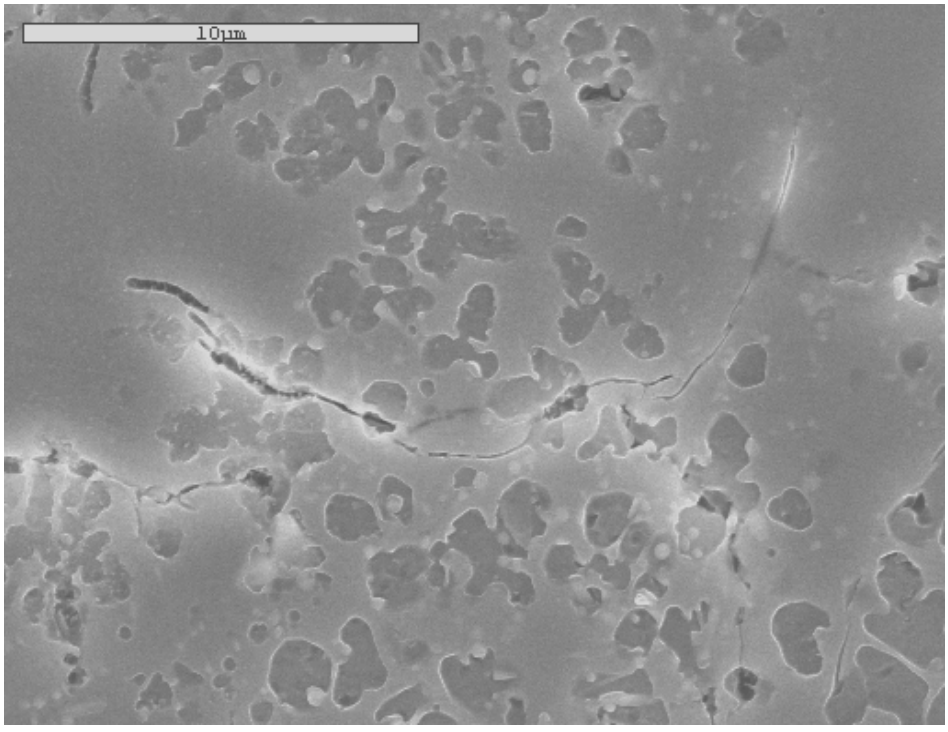

D

Figure 4-3. Continued

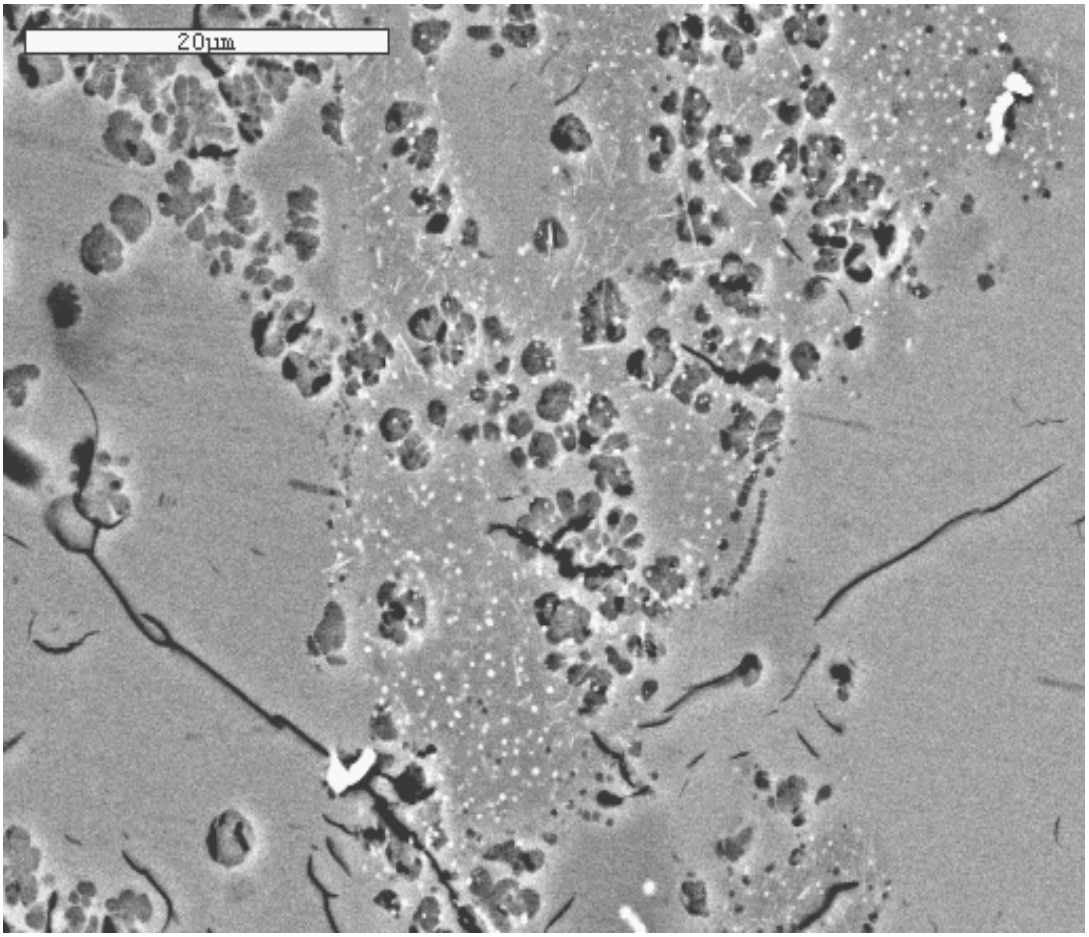

A

Figure 4-4. Image J Analysis program masking process for IPS d.SIGN. A) SEM image of IPS d.SIGN at 2000K etched for 10 seconds with 3% HF, showing flourapatite crystals and clusters of leucite crystals. B) Same SEM image as in 4-4A, this time, highlighting the leucite crystals in red, further differentiating them from the fluorapatite crystals. C) The same image using different masking technique, this time highlighting leucite crystals in black, practically obliterating or “masking” the fluorapatite crystals. D) Same SEM image as 4-4A, this time masking the leucite crystals and highlighting the flourapatite crystals in the image. E) Same image as 4-4, highlighting fluorapatite but with a different contrast.

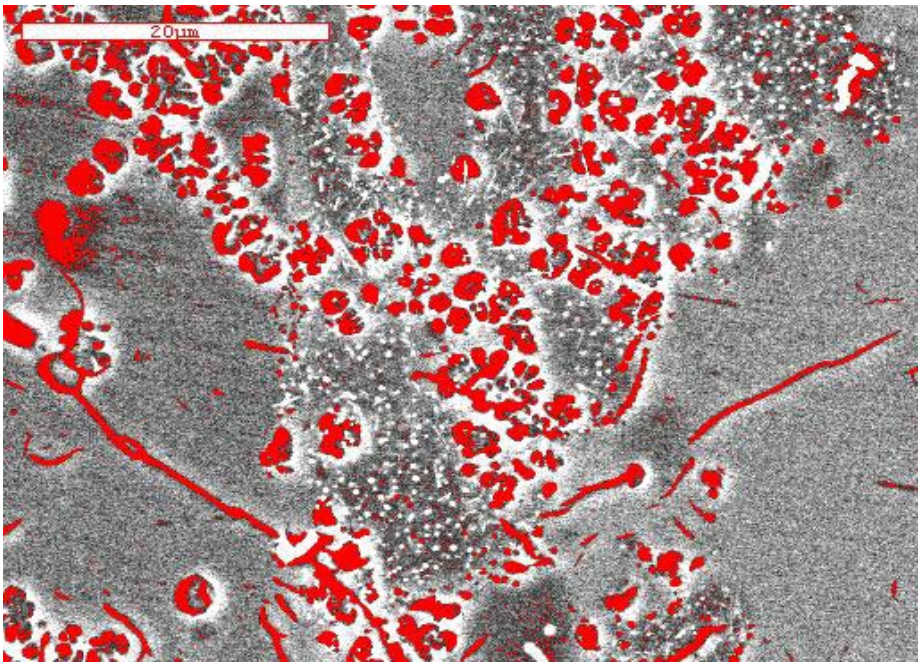

B

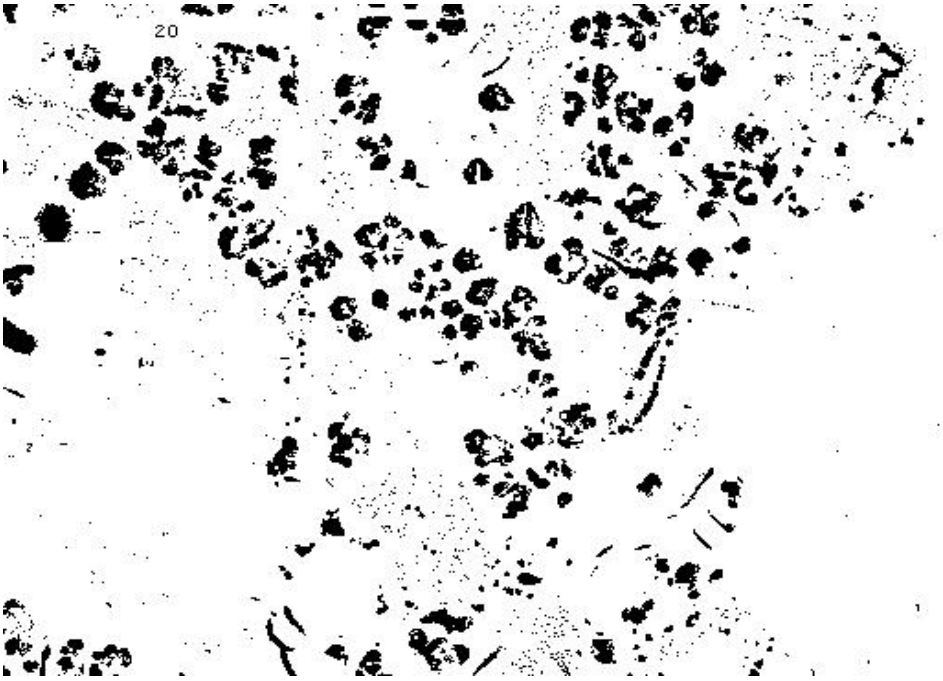

C

Figure 4-4. Continued

D

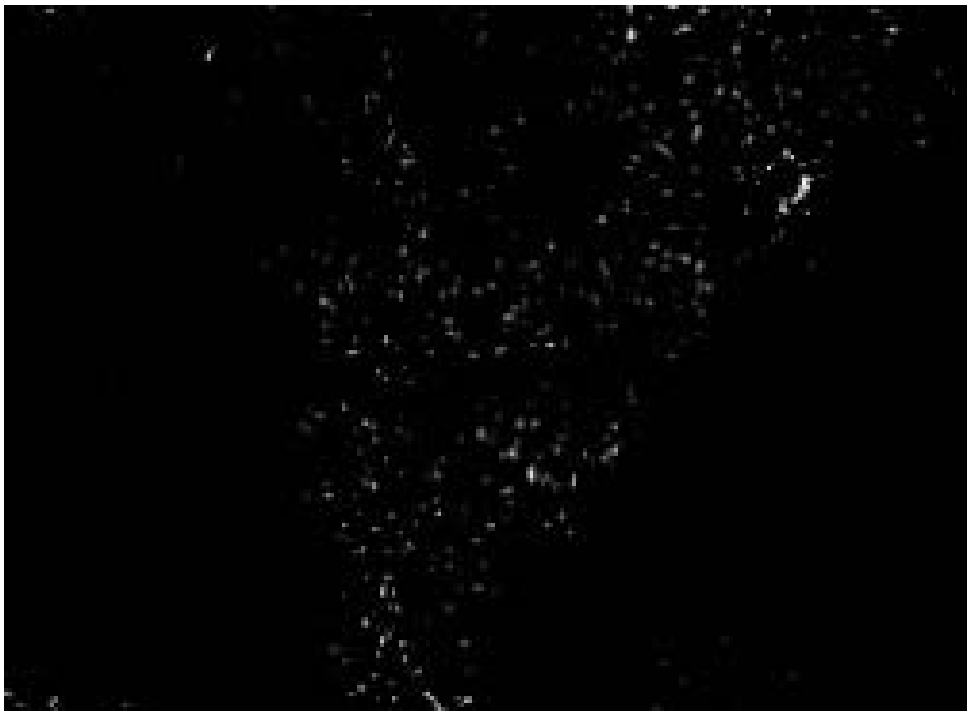

E

Figure 4-4. Continued

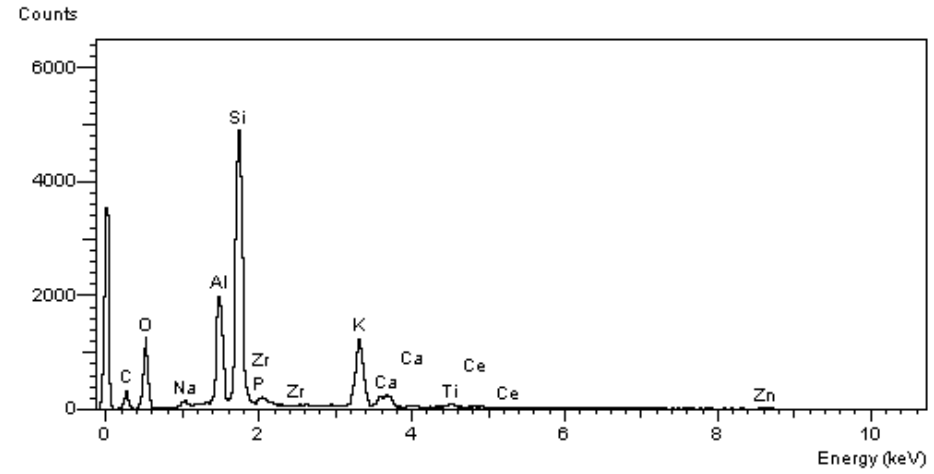

A

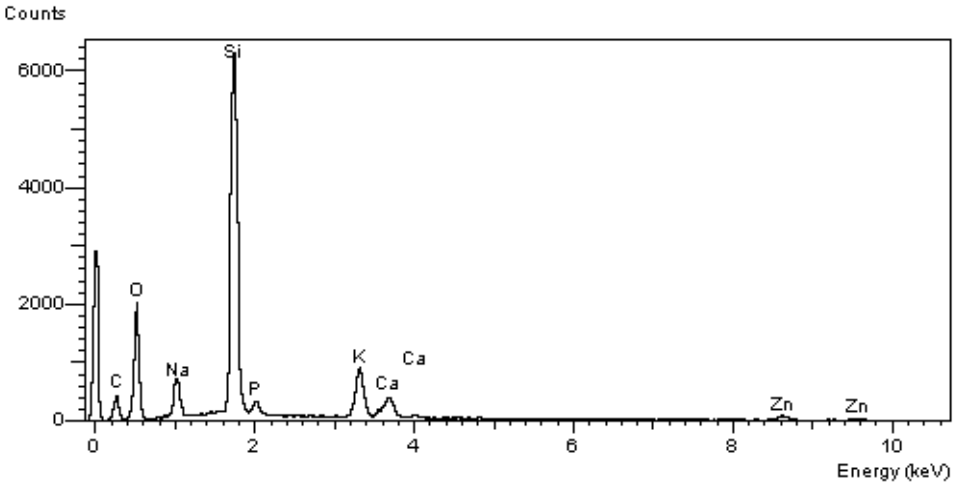

B

Figure 4-5. EDS spectra of IPS Eris depicting elemental content. A) EDS spectrum of IPS Eris located outside geometric shape. This area shows the presence of alumina, which could account for the resistance to etching. B) EDS spectrum of IPS Eris located within the geometric shape. This area seems to show a higher silica content.

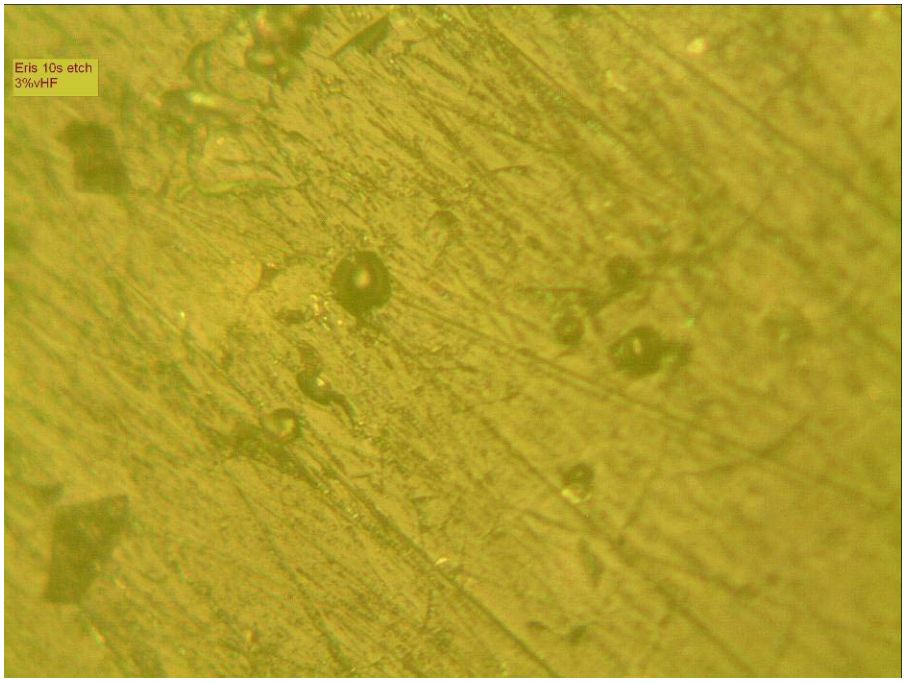

A

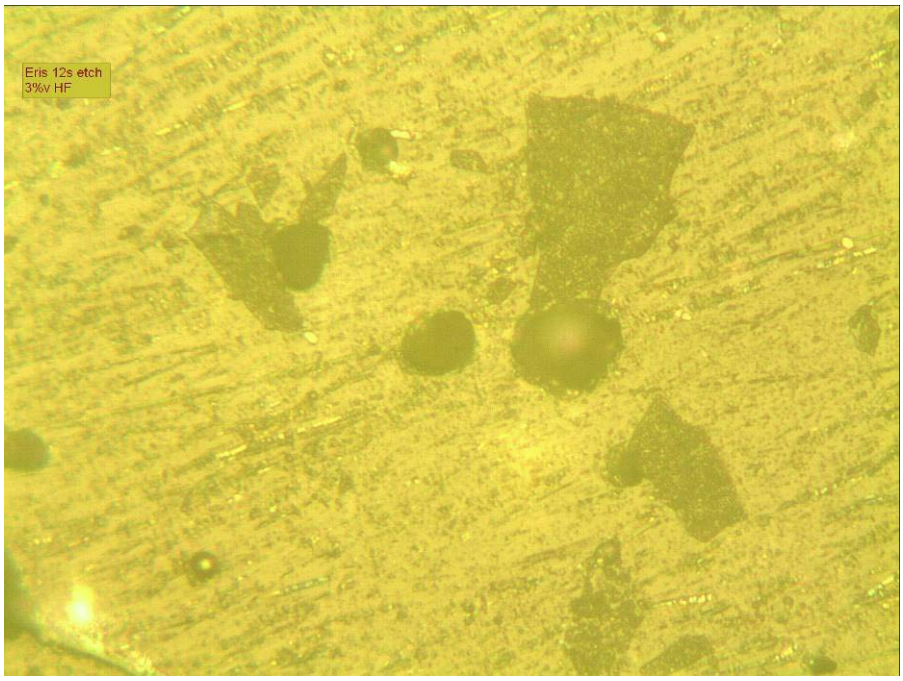

B

Figure 4-6. Optical microscopy image of IPS Eris veneering ceramic. A) IPS Eris ceramic etched for 10 seconds. B) IPS Eris ceramic etched for 12 seconds. Note the geometric shapes scattered throughout the area of the image which could signify preferential etching in these areas. C) IPS Eris ceramic etched for 15 seconds.

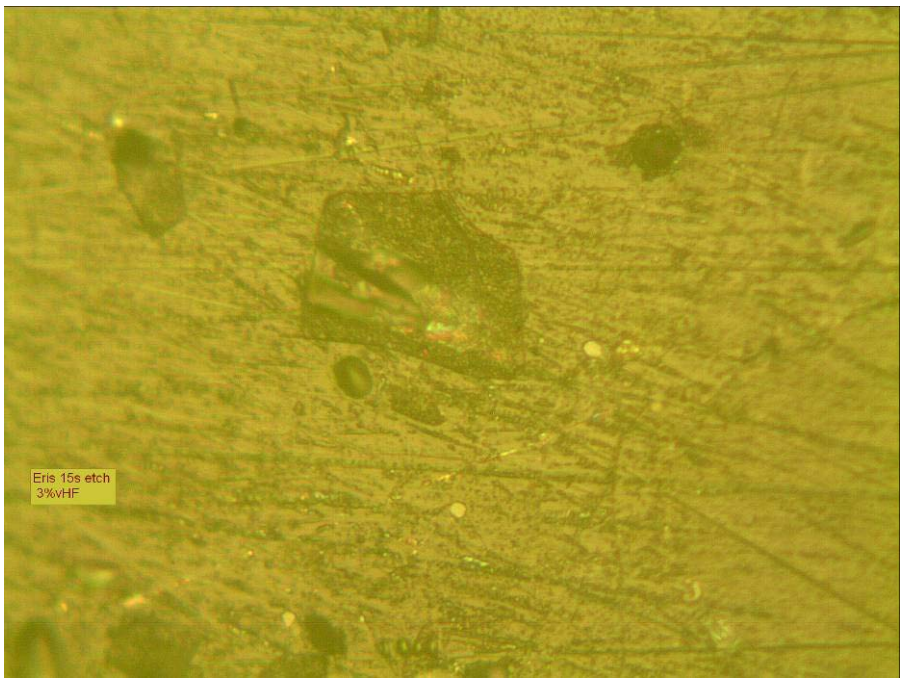

C

Figure 4-6. Continued

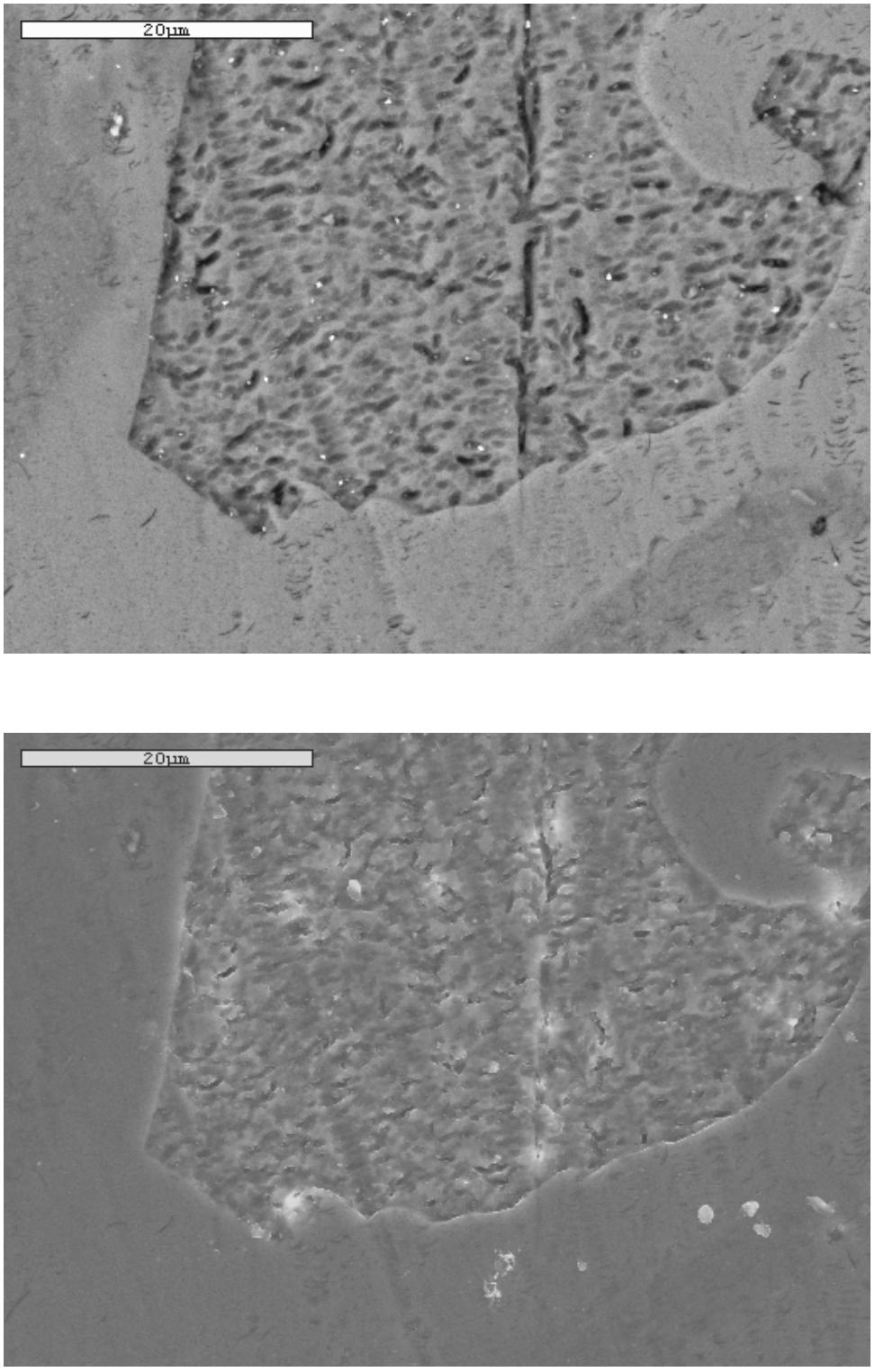

Figure 4-7. SEM images of IPS Eris veneer etched for 12 secs with 3% HF acid at 2K magnification. A) SEM image sample in backscatter mode. B) SEM image sample in secondary electron mode.

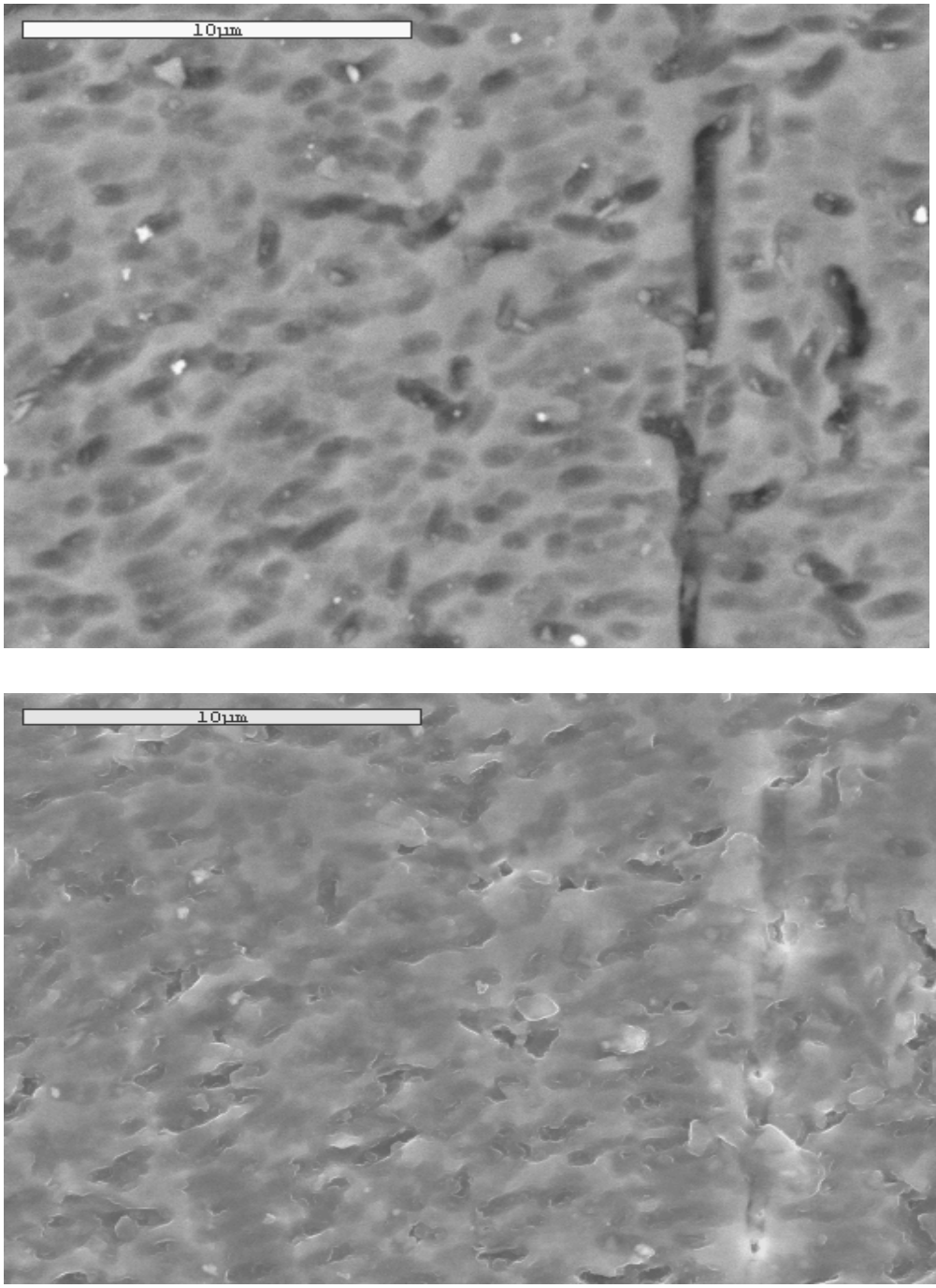

Figure 4-8. SEM image of IPS eris veneer etched for 12 seconds with 3% HF acid at 5K magnification. These images are taken inside the geometric areas, which are believed to have the preferential etching. A) Sample in the backscatter electron mode. B) Sample in the secondary electron mode.

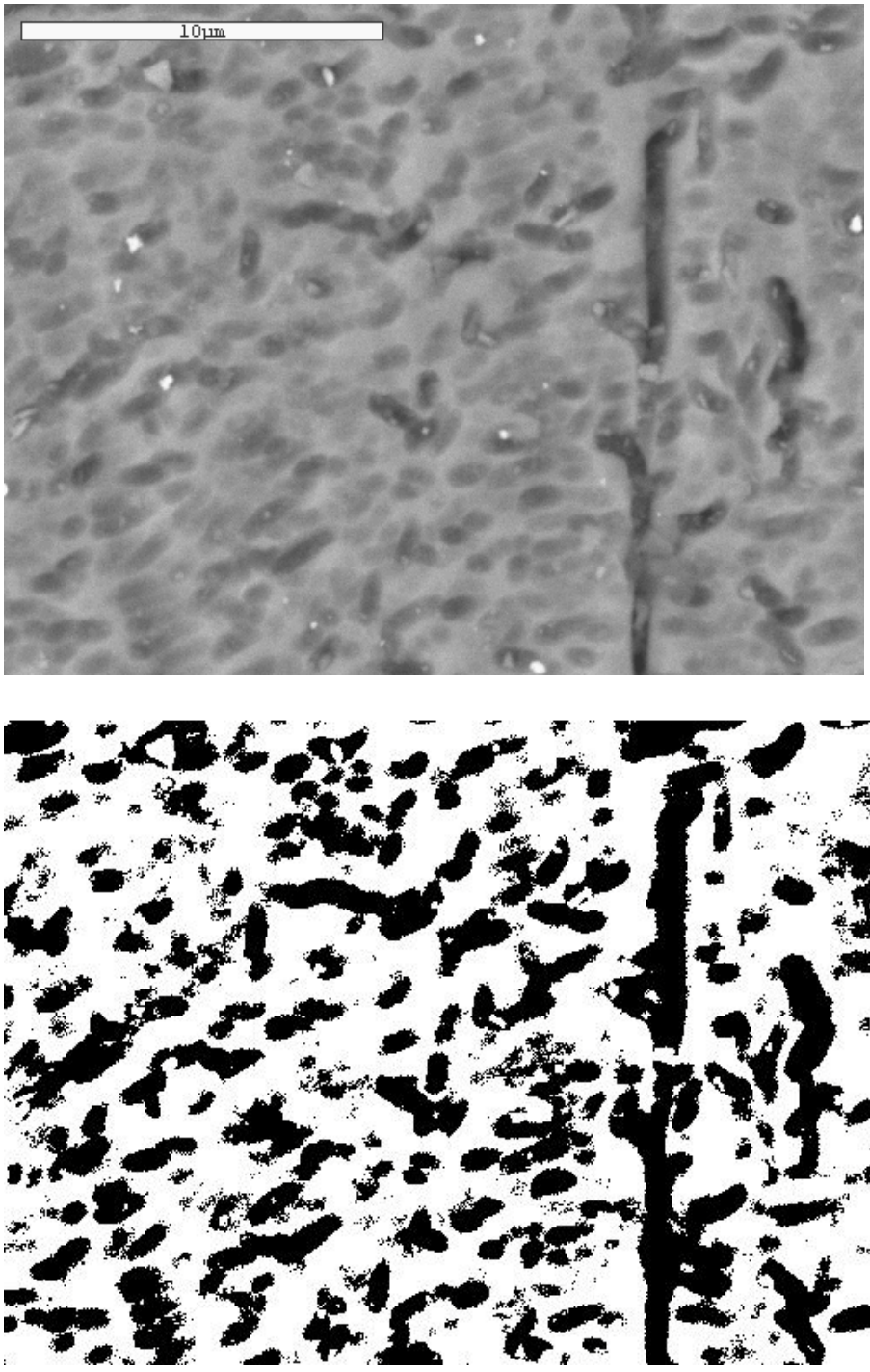

Figure 4-9. Image J analysis program masking process for IPS Eris. A) SEM image of IPS Eris at 5000x magnification, sample etched for 12 secs with 3% HF acid. This image was taken inside one of the geometric shapes throughout the ceramic that possibly showed preferential etching. B) Same SEM image in Fig. 4-9A, masked to highlight crystal content in the image to enable calculation of Vv of apatite crystals at 35.1%.

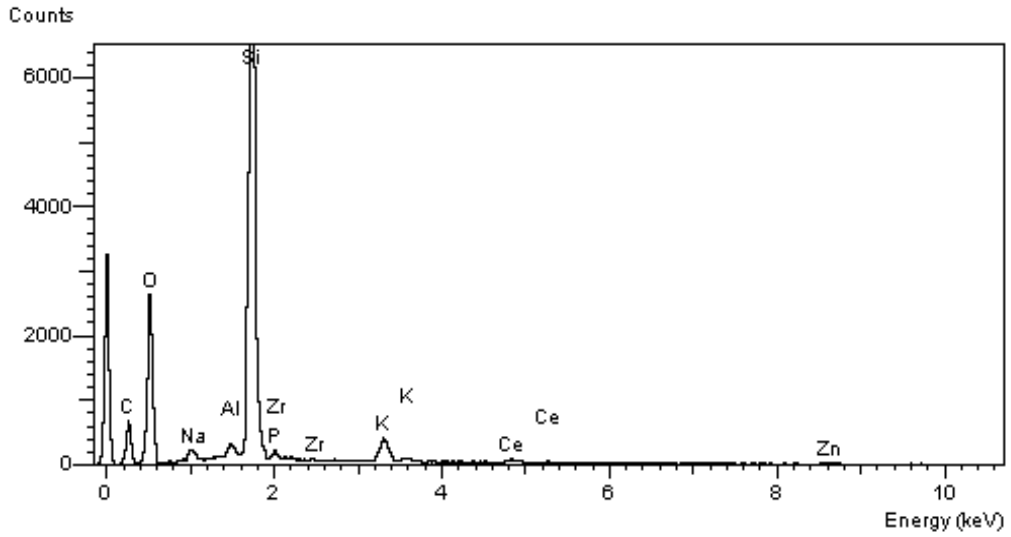

Figure 4-10. EDS spectrum of IPS e.Max Press specimen.

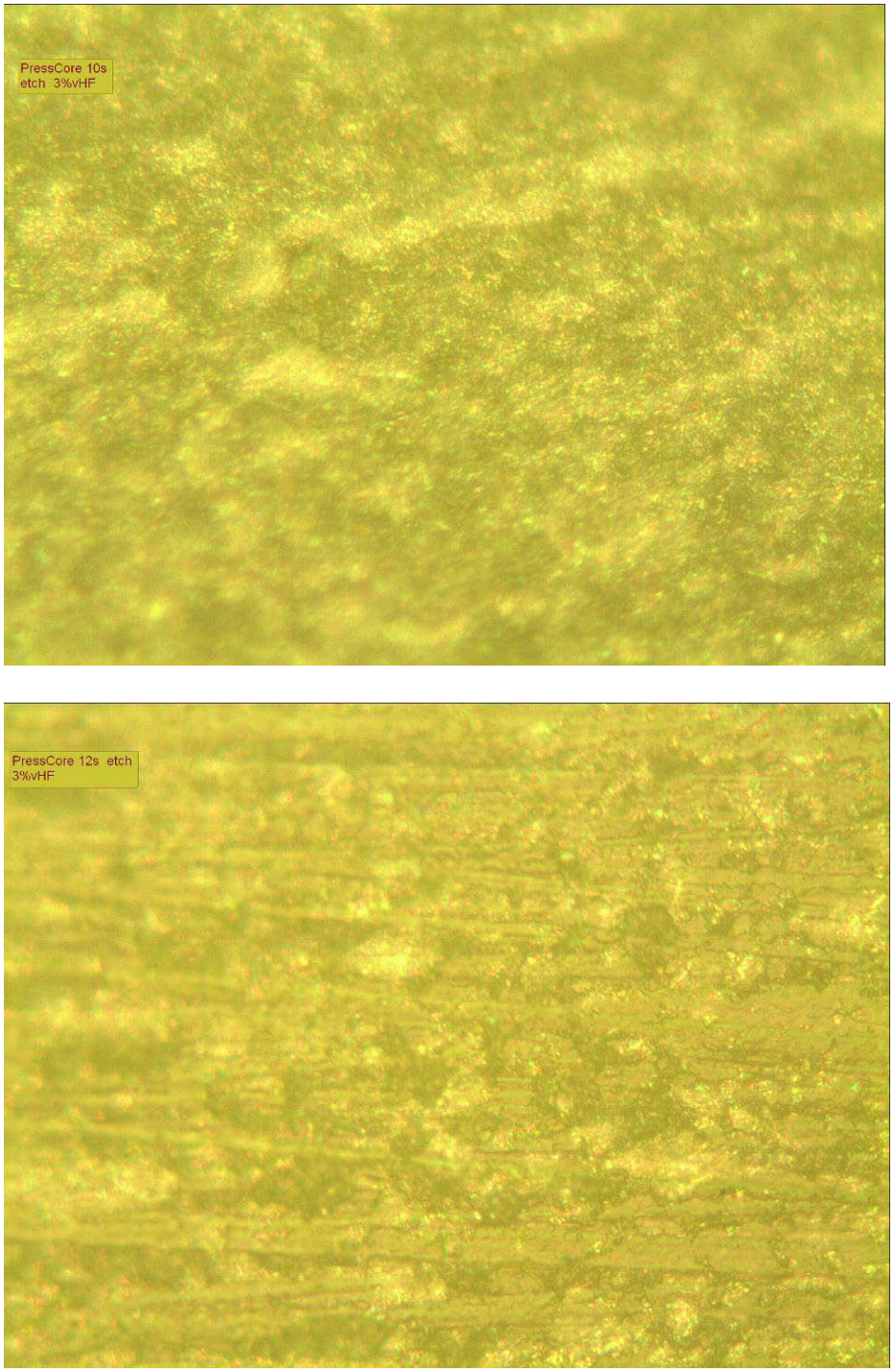

Figure 4-11. Optical microscopy image of IPS e.Max Press core ceramic etched with 3% HF acid for 10, 12 and 15 seconds. A) Optical microscopy image of IPS e.Max Press etched for 10 seconds. B) Optical microscopy image of IPS e.Max Press etched for 12 seconds. C) Optical microscopy image of IPS e.Max Press etched for 15 seconds.

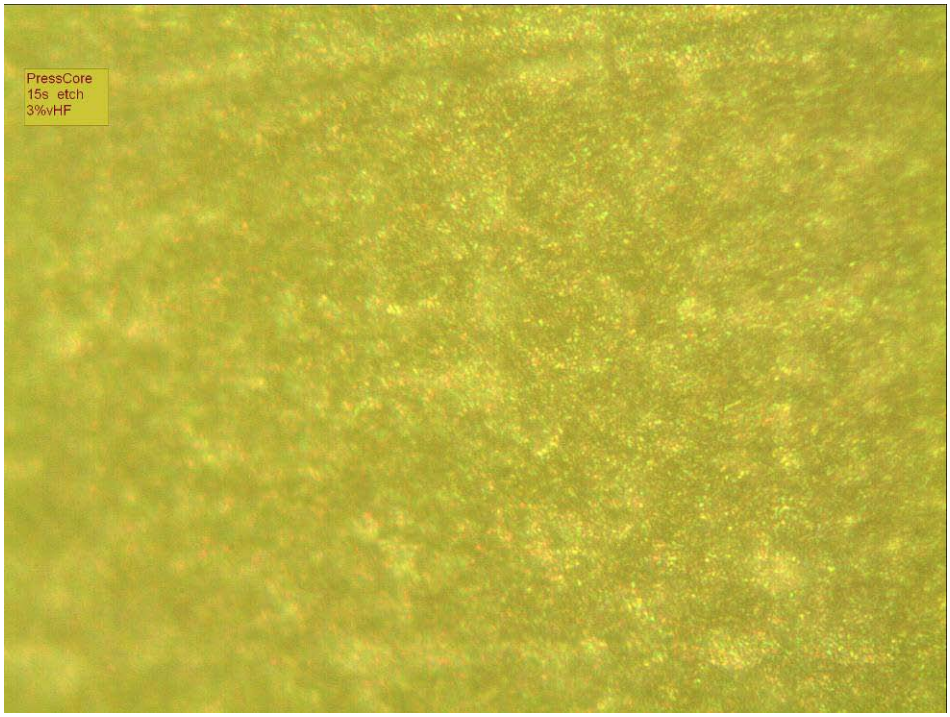

C

Figure 4.11. Continued

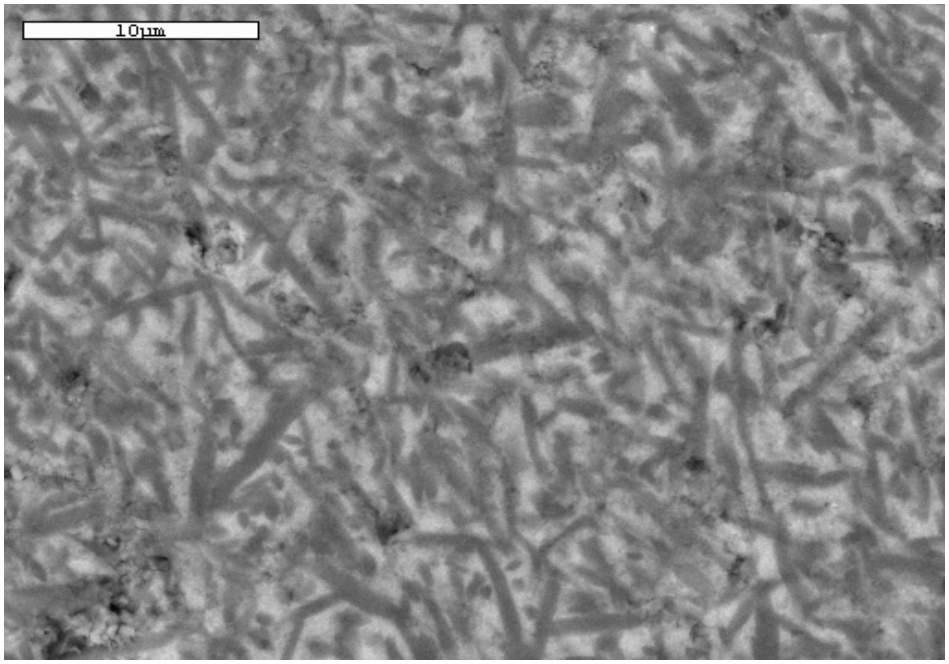

Figure 4-12. FESEM image of IPS e.Max Press specimen etched for 12 seconds with 3% HF acid at 5K magnification showing needle-like lithia disilicate crystals.

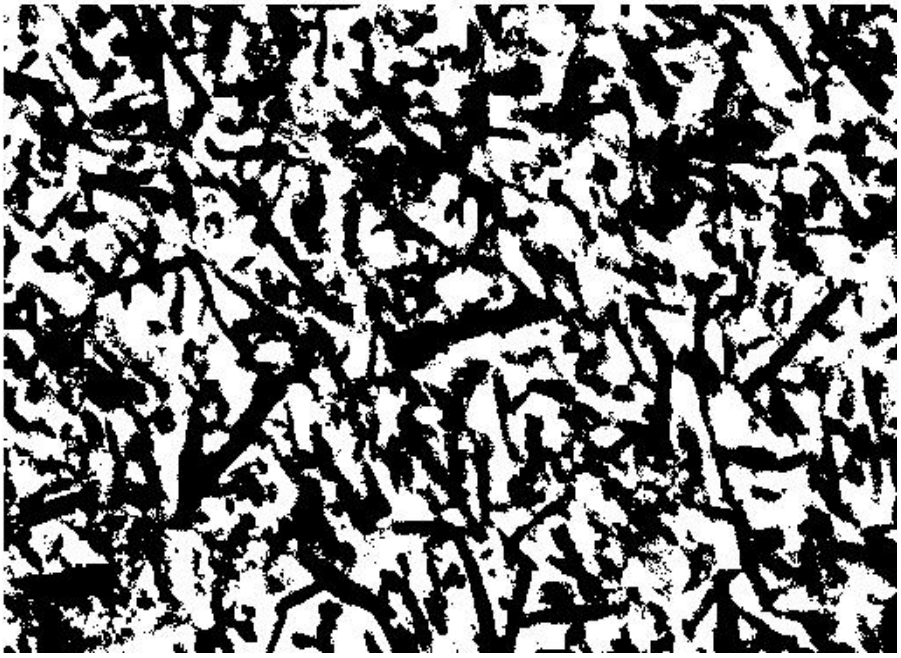
Figure 4-13. FESEM image of IPS e.Max Press in Figure 4-12 processed by Image J software.

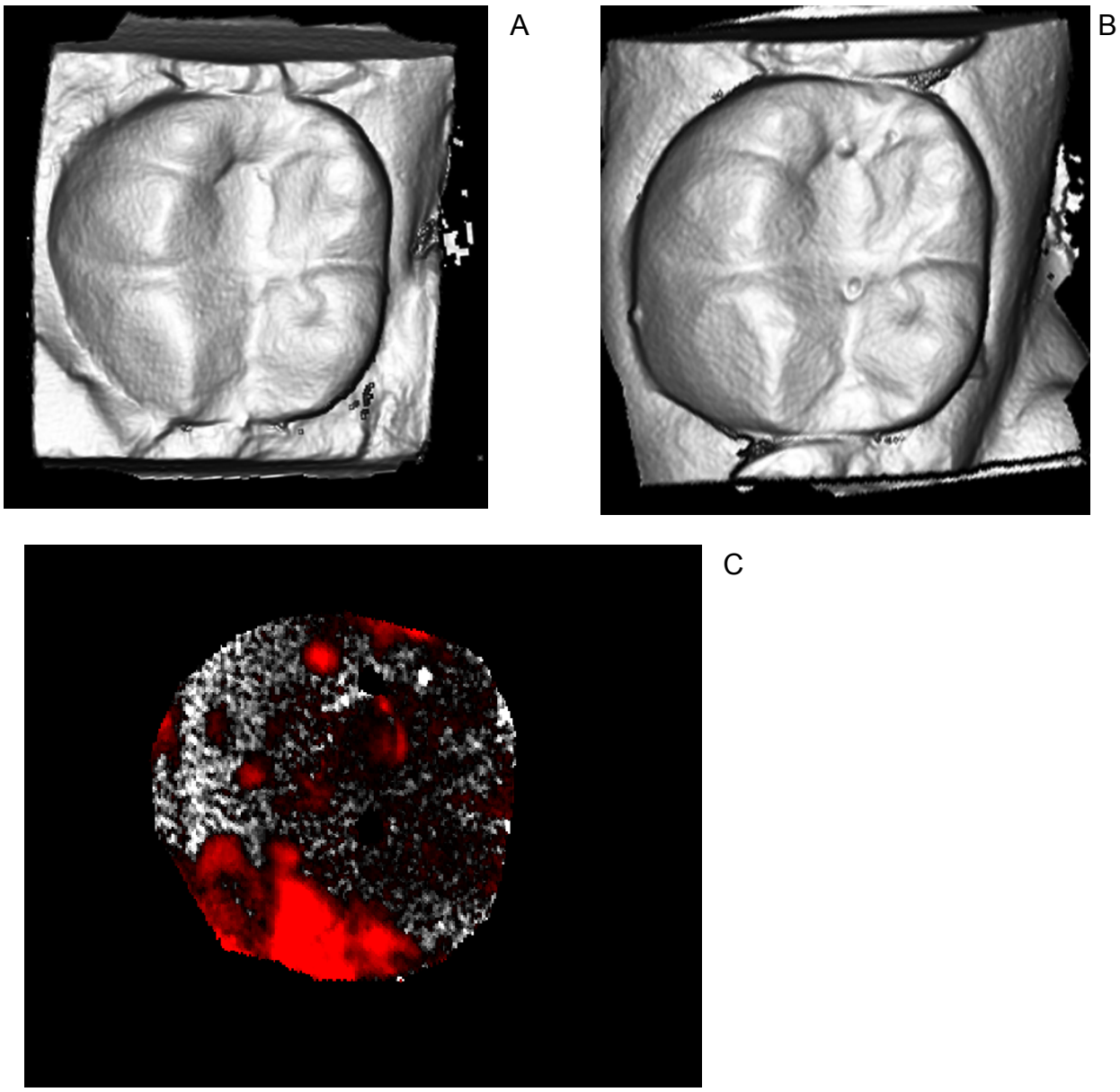

Figure 4-14. Scanned images of lower left first molar with Eris veneer. A) Baseline after cementation. B) Recall image after one year. C) Superimposed image where red shows the most wear. Note the wear circumscribed in yellow in Fig. 4-14B and the relationship with the red areas in Fig. 4-14C.

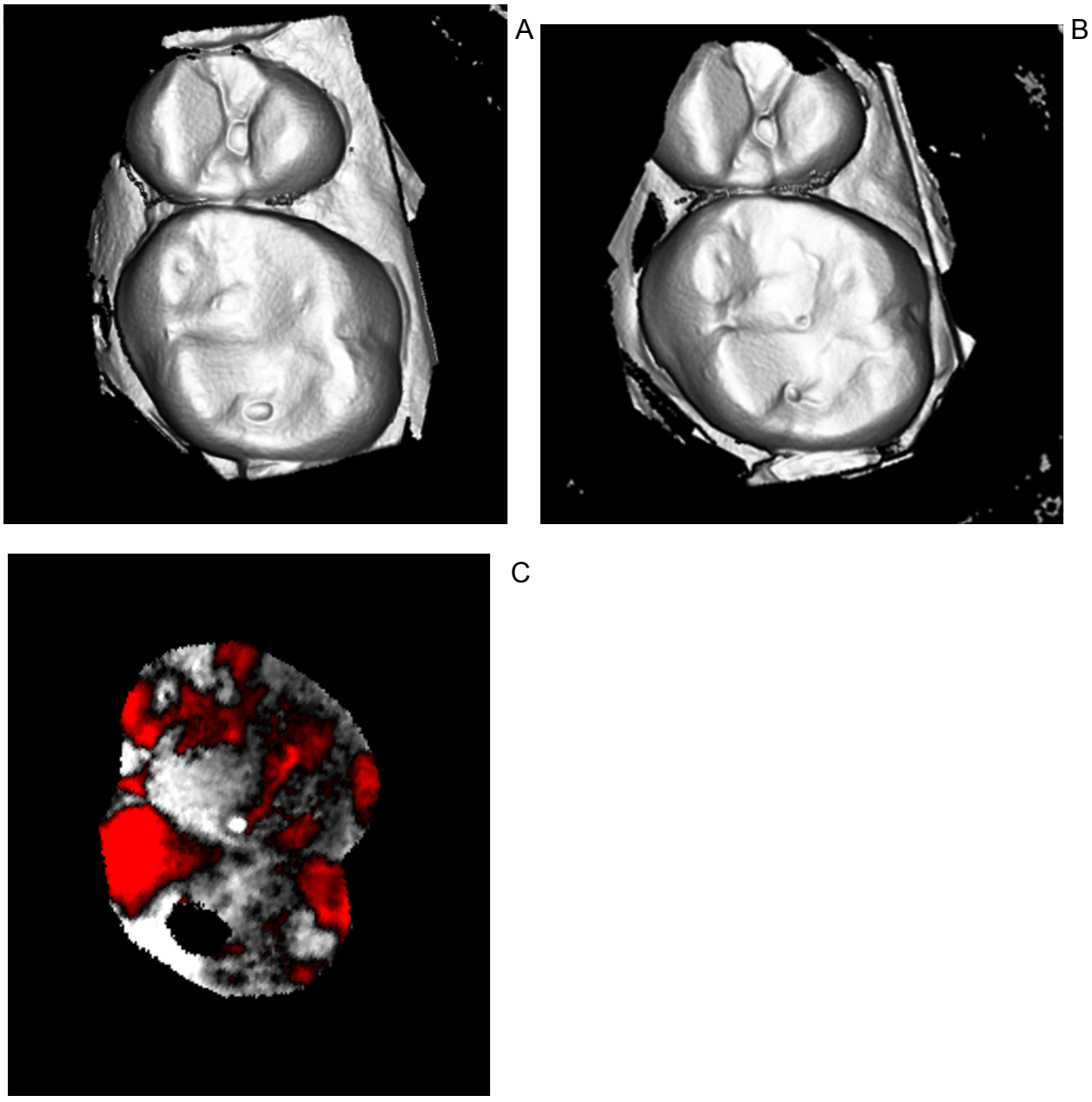

Figure 4-15. Scanned images of a maxillary right first molar opposing a crown. A) At baseline. B) After one year. C) Superimposed differential image. Note wear on buccal and lingual cusps after one year shown in Fig 4-15C in red.

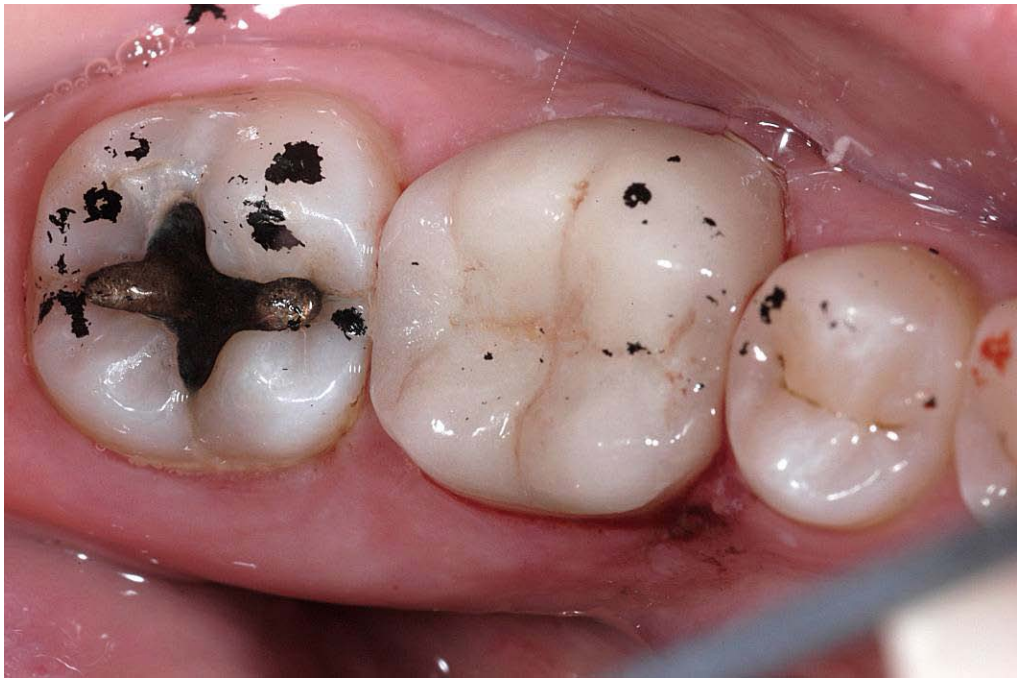

A

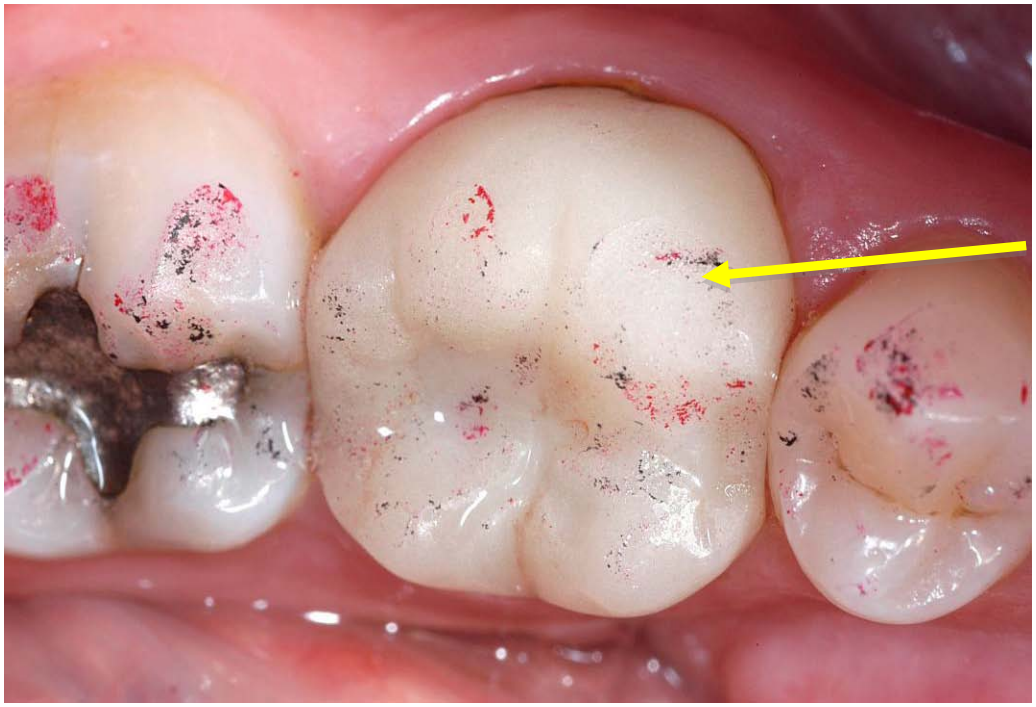

B

Figure 4-16. Clinical pictures of the mandibular left first molar made from IPS Eris. A) At baseline. B) At one year recall. Note excessive roughness on buccal surface with possible veneer fracture with yellow arrow.

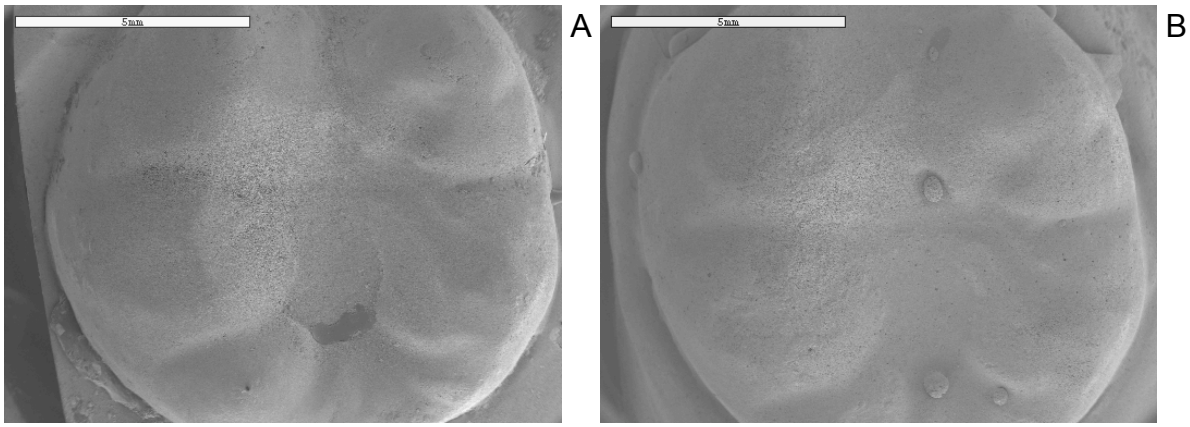

Figure 4-17. SEM images of same mandibular molar made from IPS Eris at 10x magnification. A) Baseline. B) At one year recall.

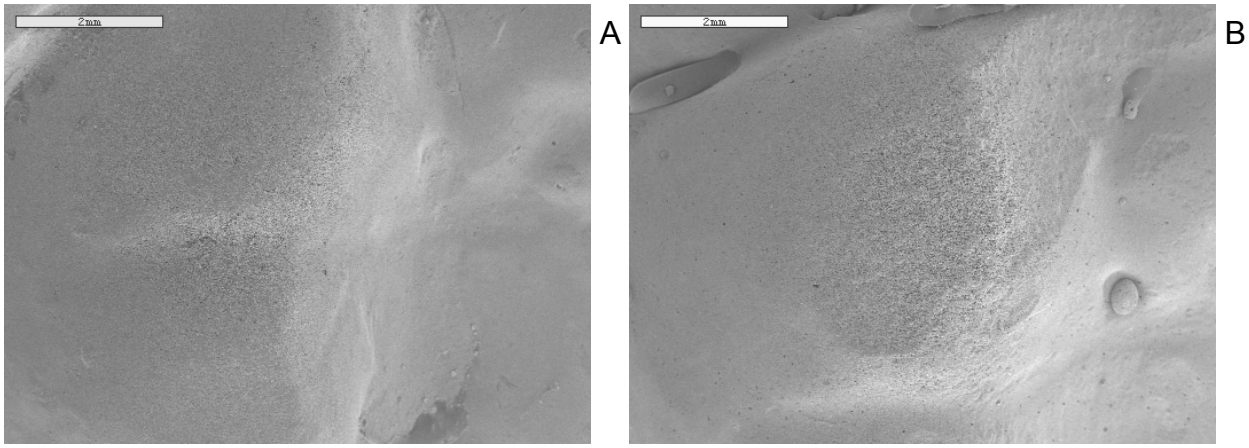

Figure 4-18. SEM images of same mandibular molar made from IPS Eris at 15x magnification focusing on mesiobuccal cusp wear. A) Baseline. B) At one year recall.

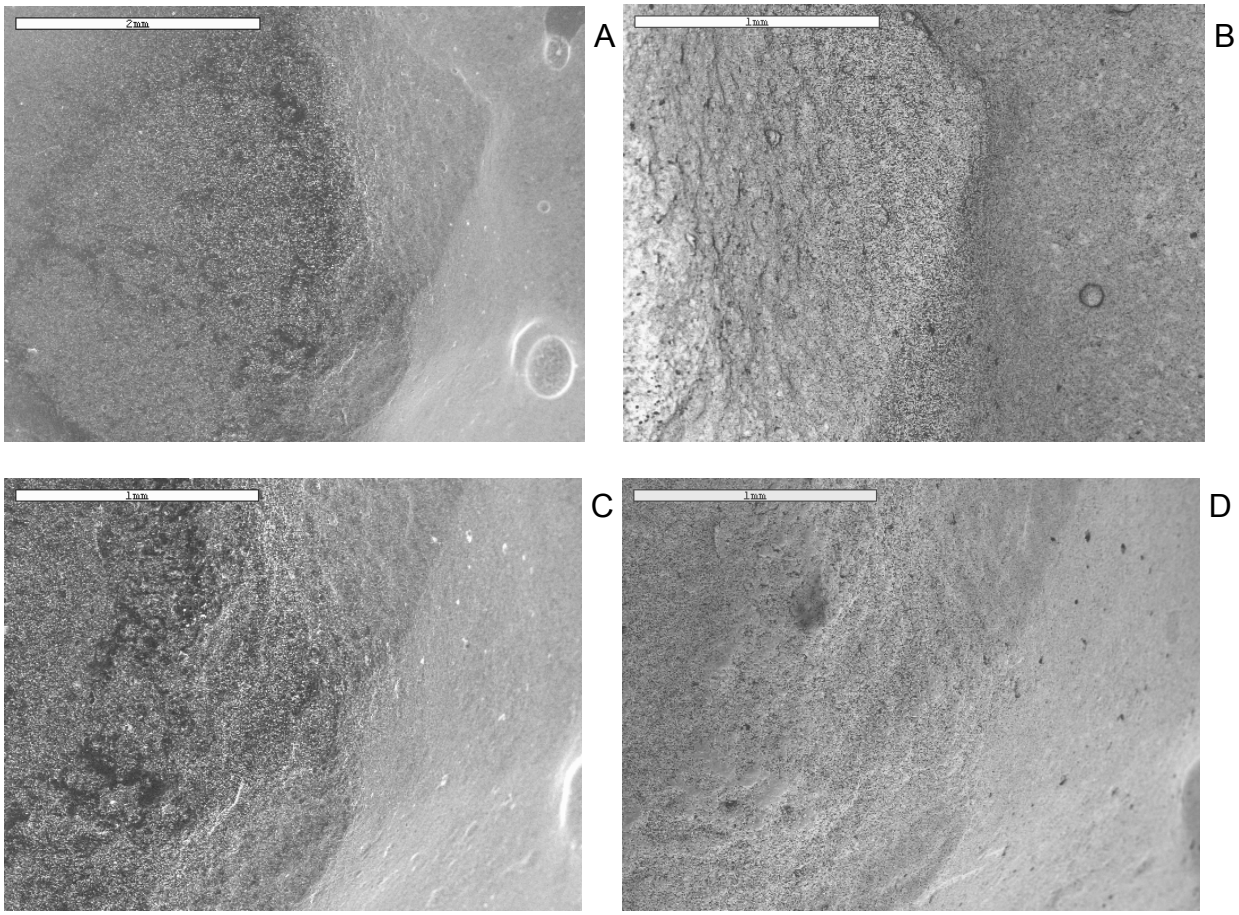

Figure 4-19. SEM image of same mandibular molar made from IPS Eris at one year at 25x magnification. A) Focused on mesiobuccal cusp. B) Focused on mesiobuccal cusp from another angle. Notice the ledge on the middle of the image demarcating where the wear occurred. C) Same image showing wavy patterns originating from the left side and ending on the marked ledge. D) Same image showing another angle of the wavy ridges, possibly indicating a site of fracture somewhere on the surface.

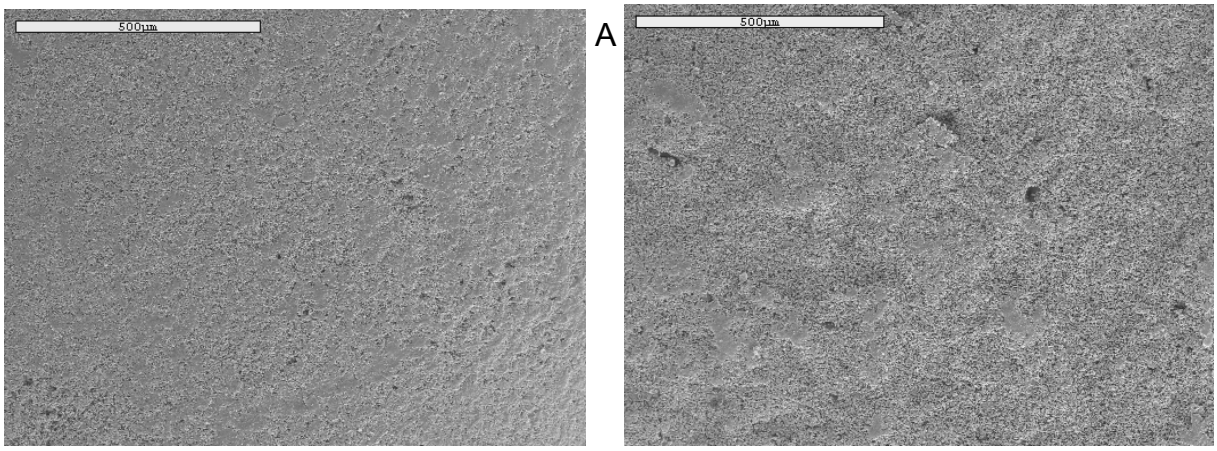

Figure 4-20. SEM images of same mandibular molar made of IPS Eris at 100x magnification. A) Baseline. B) At one year recall. Note roughened surface of 4-20B.

A

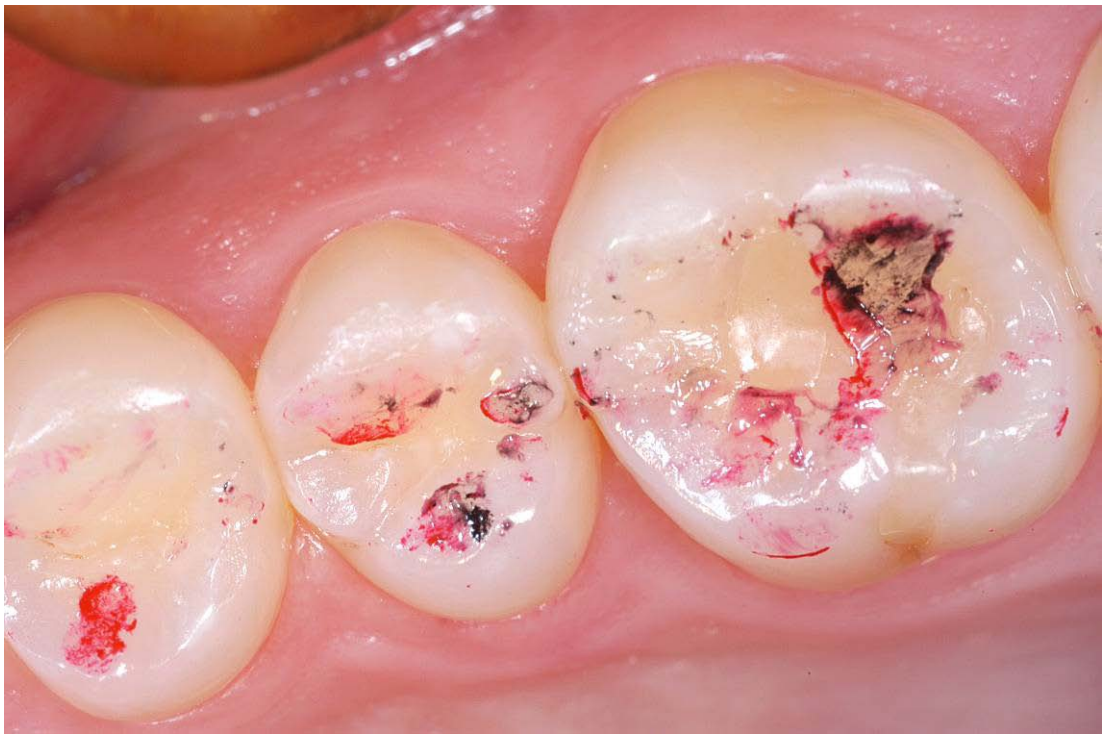

B

Figure 4-21. Clinical images of maxillary left first molar enamel opposing Eris crown. A) Baseline. B) At one year recall.

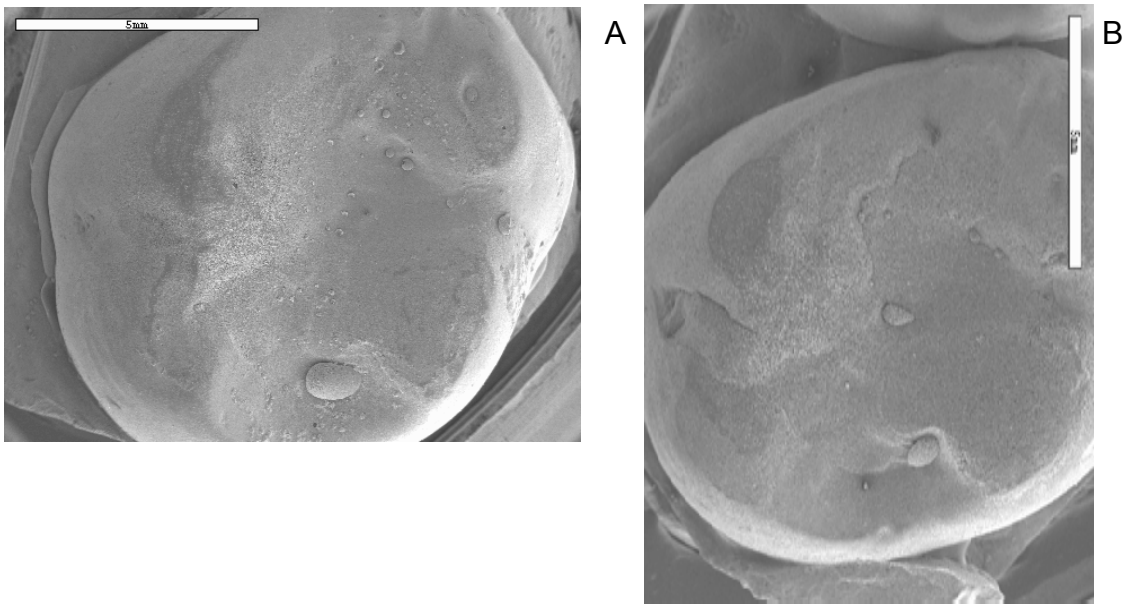

Figure 4-22. SEM images of same maxillary molar opposing IPS Eris at10x magnification. A) Baseline. B) At one year.

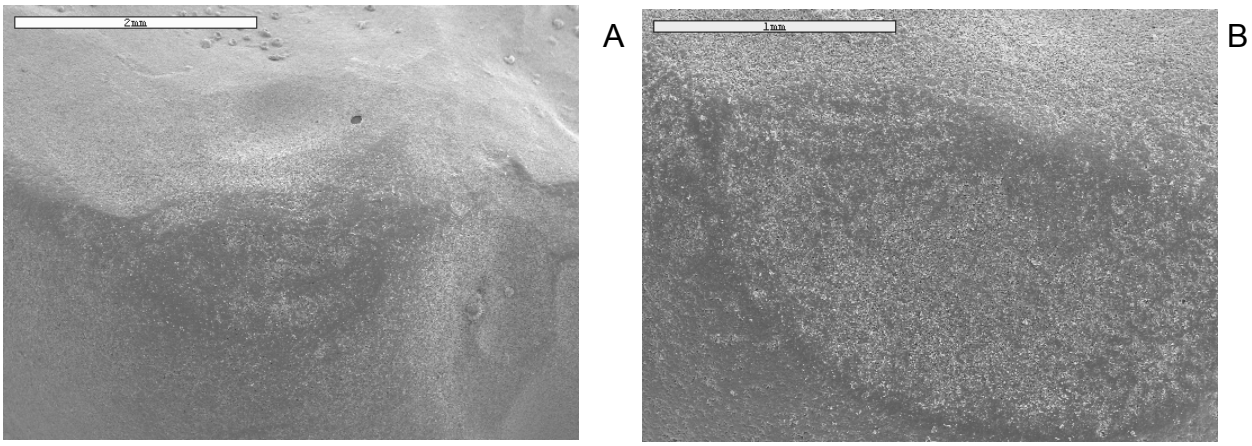

Figure 4-23. SEM images of same maxillary molar opposing IPS Eris tooth at 25x magnification. A) Baseline. B) At one year. Note definition on the wear facet after one year.

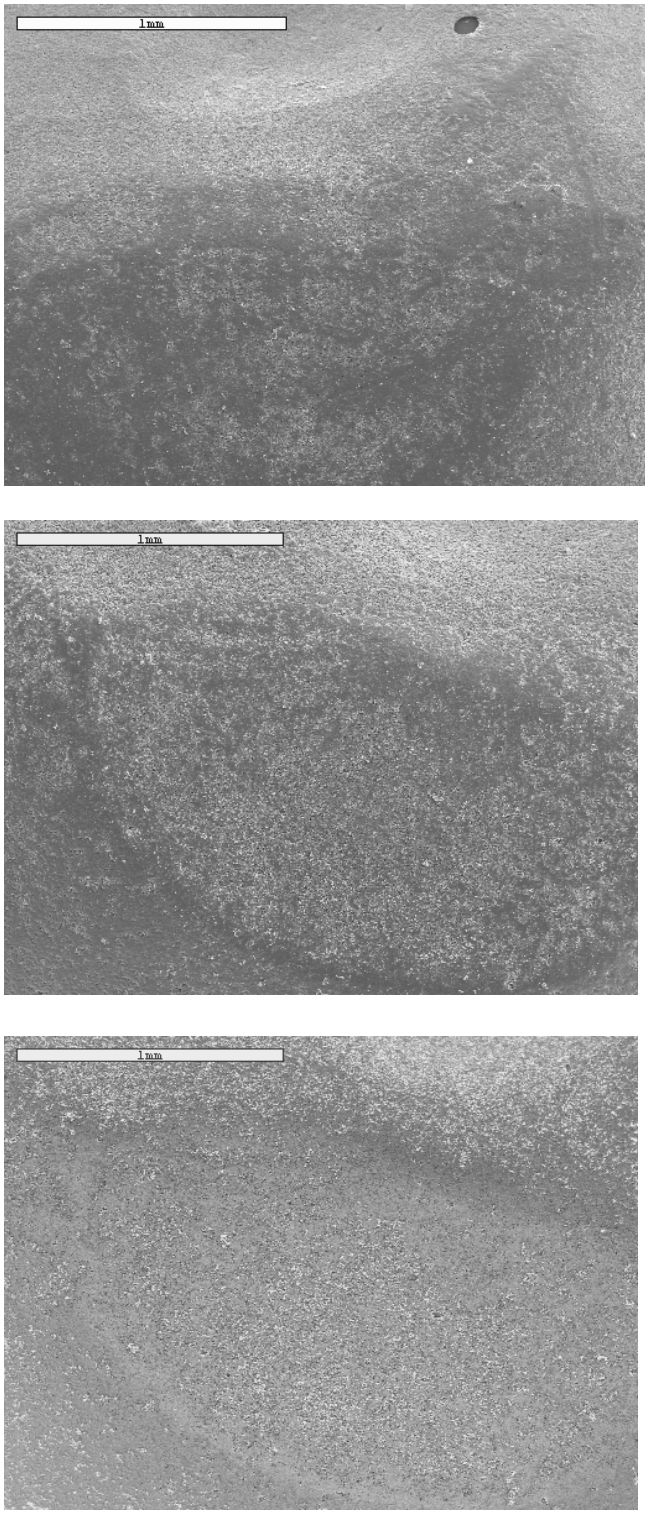

Figure 4-24. SEM images of same maxillary molar opposing IPS Eris at 50x magnification. A) Baseline. B) One year. C) Backscatter emission mode for one year.

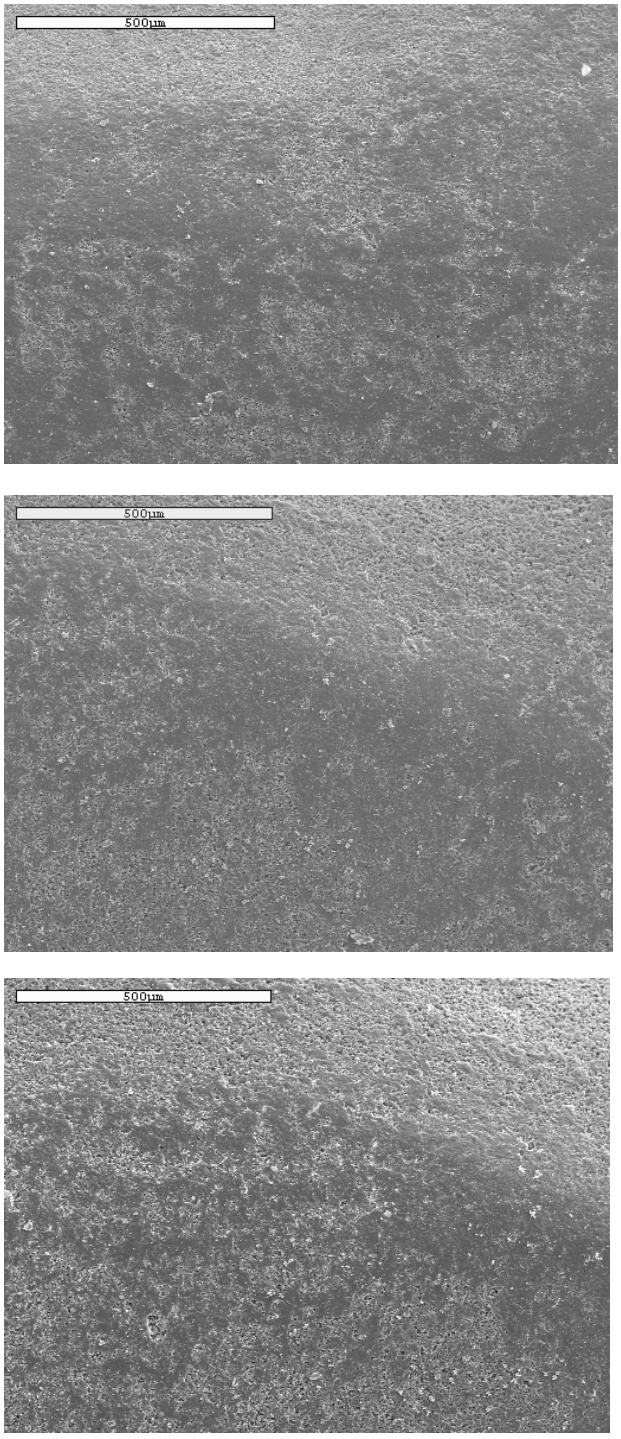

Figure 4-25. SEM images of same maxillary molar opposing IPS Eris at 100x magnification. A) At baseline. B) One year. C) One year image using backscatter emission mode.

CHAPTER 5
DISCUSSION AND CONCLUSION

Discussion

This study is unique because it analyzed wear of enamel opposing ceramic in an *in vivo* setting. Ceramic can be a very abrasive material and can cause accelerated wear of the opposing teeth. Previous research studies analyzed wear of ceramic *in vitro*. To date, only one study has been published showing that the normal yearly wear between enamel versus enamel was 88.3 μm *in vivo* [58]. In contrast, the results of our study indicate that ceramic wear is comparable to the enamel antagonist wear with a mean annual wear of 48.7 μm for ceramic and 54.9 μm for enamel. The wear values also fall below the normal yearly wear value of 88.3 μm between enamel versus enamel surface. These results are a good indication that this formulation of ceramics offers a less abrasive restorative option.

There is considerable debate over which value of wear is more significant in a clinical setting. The 3D Laserscanner delivers two sets of data, one for volumetric wear and the other for maximum wear. Volumetric wear accounts for the total volume wear in a given area, in this case, the occlusal surface of the tooth. While this value may be of interest, volume wear may be misleading and therefore not significant. Take the example of a mandibular first molar, which probably has one of the largest occlusal surface areas of approximately 56 mm^2 [59]. A given volumetric wear value of 250 μm^3 may seem large but when divided over the surface area, the value amounts to a wear value of 4.46×10^{-6} μm wear per μm^2 over a year, which seems negligible. However, a maximum wear of 250 μm over one particular area could prove to be very harmful and detrimental to the orofacial system. The two *in vivo* studies [14, 15], which examined

wear using a 3D Laserscanner reported wear as a volumetric loss. We believe that maximum wear is the more significant value that needs to be reported.

This study is also unique because we analyzed the wear on the contralateral side as the control enamel versus enamel wear. Unexpectedly, the crown contralateral antagonist teeth demonstrated the greatest amount of wear out of the four groups (crown, crown antagonist, crown contralateral tooth and crown contralateral antagonist). While crossover studies are expedient, the results of these studies should be viewed very carefully as the experimental side may "contaminate" or unduly affect the control side and alter the results. In this case, a three-body wear could be the cause of increased wear on the CCA group. This increased wear may be due to small glass particles, which are introduced in the mouth as the ceramic wears down. These particles can act as a third body foreign object, causing accelerated wear of the contralateral teeth. Another interesting finding is that CCA demonstrated the most variability in wear. We can postulate that the possibility of masticatory posturing could exist, whereby the subject either consciously or unconsciously favors chewing on the opposite side of the crown, although this theory fails to explain why overall the crown contralateral teeth showed the least wear. The significant effect of bite force upon separate analysis of CCA wear indicates that bite force may not be distributed uniformly across the entire occlusal surface. Future studies need to develop a device that could measure bite force for the left and right areas of the mouth to determine if posturing does exist to compensate for the new prosthesis.

This study is also comprehensive in analyzing the different characteristics of ceramics and how they relate to wear of ceramic and opposing enamel. To date, this

study is the only one that has analyzed the microstructure of the ceramic materials used in a clinical study to correlate the results of clinical wear. The two veneering ceramics and one core ceramic used in this study exhibited no significant difference in their wear of the opposing enamel despite notable differences in their microstructure and physical properties. The physical properties were also different in that IPS e.Max Press exhibited the highest fracture toughness of 2.35 MPa•m ^{½} and, although not statistically significant, possibly the most resistance to wear.

The ceramics have similar elemental content with a predominance of silicon although they all have different crystal structures and grain sizes. The microstructural findings are consistent with other studies, which analyzed at the microstructure of the same materials [54, 60, 61]. In our analyses, we confirmed the presence of lithia disilicate crystals in IPS e.Max Press through the presence of silicon and lithium in EDS as well as through a comparison of SEM images to previous studies. Also, there was confirmation of the fluorapatite crystals we believe to be present in IPS Eris. In the study by Holand et al., [54], they described the presence of apatite glass-ceramic crystals which are seen as white geometric shaped islands in SEM images. These are consistent with the geometric shapes we saw on SEM images, which we believe to be areas that are more susceptible to etching. Next, there are “specific numbers of very finely dispersed apatite crystals that have been precipitated in the glassy matrix of the glass-ceramic” [54], again describing the fine crystals we saw on higher magnification. Although there was no evidence of fluoride in EDS spectra, the presence of potassium, calcium and phosphorus support the claim that there are apatite crystals in the ceramic. The study further describes the possibility of these apatite crystals being etched away

from the surface, leaving deficits or craters where the crystals existed, which is what we believe we viewed for fluorapatite. In another study, the evolution of IPS d.SIGN was described [60]. The microstructure of the veneering ceramic was outlined in detail pertaining to the controlled nucleation of both the apatite and leucite crystals. This study noted that leucite existed in single crystals although twinning was observed. In our study, we noted an abundance of leucite agglomerations, which is probably more significant than twinning. This observation could be related to differences in firing temperature and heat treatments, which could have affected crystal nucleation and other properties [50, 62].

There were several challenges that were encountered during the microstructural analyses of the ceramics. First, the lack of homogenous distribution of the crystal phase made it difficult to analyze crystal size with certainty. As such, the crystal size values were not included in the statistical model. Leucite in particular tends to have different sized agglomerations and the boundaries of single crystal structures were difficult to detect. Second, there was predominant overlapping of crystals, particularly with the lithia disilicate crystals. Since the overlapping may add considerable strength to the ceramic as evidenced by the high fracture toughness, this characteristic also added a greater challenge to grain size analysis. One of the original hypotheses of our study was to determine whether a larger interparticle spacing reduced the wear damage on opposing enamel. Due to the same challenges that were encountered for grain size determination, we decided to include an alternative hypothesis for hardness and not include crystal size values in the statistical model. We could have alternatively used the

values for volume fraction of crystals, but this would only have told us whether a higher crystal content has any effect on the wear of opposing enamel.

Although not statistically significant, the results also show that IPS e.max Press is a more wear resistant material. This finding could be explained by the fact that IPS e.Max Press also has the highest fracture toughness of the three ceramics used in this study. Since the fracture toughness is the intrinsic property that measures the resistance to crack propagation in ceramic, fractures on the surface leaving harder crystals and rougher surfaces are minimized. Interestingly, the higher fracture toughness did not show any difference in the wear of the opposing enamel. The lithium disilicate microstructure, which is densely packed and overlapping, also accounts for the increased strength and higher fracture toughness of this material.

The SEM image of one of the representative crowns made of IPS Eris showed one of the roughest surfaces of all the crowns in the study. This finding was made even more apparent by the patient who described the roughness with her tongue as like “gritty sandpaper”. Although not significant in terms of enamel wear, IPS Eris had the lowest fracture toughness among the three ceramics in the study. The next phase of this study will examine the surface of this particular crown through fractographic analysis to detect fractures that may have occurred on the surface, which could explain the excessive roughness. Due to the lower fracture toughness of IPS Eris, the possibility of crack propagation is higher, which could lead to catastrophic failures or fractures of the restoration. Another factor to be examined is the chemical solubility of the glassy phase. A high solubility of the glassy phase can also contribute to roughness

of the surface through dissolution of the ceramic, possibly increasing wear of the opposing enamel.

IPS e.max Press has a higher fracture toughness and densely packed crystals [63, 64]. This study shows that IPS e.max Press as potentially being more wear resistant than other ceramics. However, no other factors mentioned above contributed to increased wear of the opposing enamel or of the other areas in the mouth.

Conclusion

This study shows that no correlation exists between bite force and the amount of wear, although the effect of bite force is more clearly seen when the wear of the contralateral antagonist teeth is examined separately. Additionally, there is no significant difference in the wear of opposing enamel by two veneering ceramics and one core ceramic despite the differences in microstructure, fracture toughness and hardness of the ceramic restorations opposing them. However, microstructure and fracture toughness do influence the wear resistance of the ceramic material as evidenced by the higher wear resistance of IPS e.Max Press.

APPENDIX
MANUFACTURER'S RECOMMENDED FIRING SCHEDULES

For all tables:

- Temperatures given in centigrade
- T = Top temperature
- B= Idle temperature
- t= Temperature rise rate
- H = Hold time
- V1 = Vacuum on
- V2 = Vacuum off

A-1. IPS d.SIGN veneering porcelain for metal-ceramic crowns

	T	B	S	t	H	V_1	V_2
First and second opaque firing	900	403	6 min	60	1min	450	899
Shoulder Firing	890	403	6 min	60	1 min	450	889
First dentin and incisal firing	870	403	10 min	40	1 min	450	869
Corrective firing	870	403	4 min	60	1 min	450	869
Add-on material Firing	750	403	4 min	60	1 min	450	749
Glaze firing without glazing paste	870	403	4 min	60	0.5-1 min	450	869
Glaze firing with glazing paste	830	403	4 min	60	1-2 min	450	829

A-2. IPS Eris veneering porcelain for all-ceramic crowns

	T	B	S	t	H	V_1	V_2
Foundation firing	765	403	6 min	55	1min	450	764
Dentin, incisal and impulse material firing	765	403	6 min	55	2 min	450	764
Universal shade/stains	735	403	4 min	55	1 min	450	842
Universal glaze	735	403	6 min	55	1-2 min	450	734
Corrective firing	710	403	4 min	55	1 min	450	709

A-3. IPS e.Max Press core ceramic

	T	B	S	t	H	V_1	V_2
Press parameters	930	700	6 min	60	25 min	500	930

LIST OF REFERENCES

1. Clelland, N.L., et al., *Wear of enamel opposing low-fusing and conventional ceramic restorative materials.* J Prosthodont, 2001. **10**(1): p. 8-15.

2. Okeson, J.P., *Etiology and treatment of occlusal pathosis and associated facial pain.* J Prosthet Dent, 1981. **45**(2): p. 199-204.

3. Heintze, S.D., et al., *Wear of ceramic and antagonist--a systematic evaluation of influencing factors in vitro.* Dent Mater, 2008. **24**(4): p. 433-49.

4. Abe, Y., et al., *An in vitro wear study of posterior denture tooth materials on human enamel.* J Oral Rehabil, 2001. **28**(5): p. 407-12.

5. Clelland, N.L., et al., *Relative wear of enamel opposing low-fusing dental porcelain.* J Prosthodont, 2003. **12**(3): p. 168-75.

6. Elmaria, A., et al., *An evaluation of wear when enamel is opposed by various ceramic materials and gold.* J Prosthet Dent, 2006. **96**(5): p. 345-53.

7. Heintze, S.D., et al., *A comparison of three different methods for the quantification of the in vitro wear of dental materials.* Dent Mater, 2006. **22**(11): p. 1051-62.

8. Kadokawa, A., S. Suzuki, and T. Tanaka, *Wear evaluation of porcelain opposing gold, composite resin, and enamel.* J Prosthet Dent, 2006. **96**(4): p. 258-65.

9. Olivera, A.B. and M.M. Marques, *Esthetic restorative materials and opposing enamel wear.* Oper Dent, 2008. **33**(3): p. 332-7.

10. Suzuki, S., S.H. Suzuki, and C.F. Cox, *Evaluating the antagonistic wear of restorative materials when placed against human enamel.* J Am Dent Assoc, 1996. **127**(1): p. 74-80.

11. Mehl, A., et al., *A new optical 3-D device for the detection of wear.* J Dent Res, 1997. **76**(11): p. 1799-807.

12. Folwaczny, M., et al., *Determination of changes on tooth-colored cervical restorations in vivo using a three-dimensional laser scanning device.* Eur J Oral Sci, 2000. **108**(3): p. 233-8.

13. Perry, R., et al., *Composite restoration wear analysis: conventional methods vs. three-dimensional laser digitizer.* J Am Dent Assoc, 2000. **131**(10): p. 1472-7.

14. Suputtamongkol, K., et al., *Clinical performance and wear characteristics of veneered lithia-disilicate-based ceramic crowns.* Dent Mater, 2008. **24**(5): p. 667-73.

15. Etman, M.K., M. Woolford, and S. Dunne, *Quantitative measurement of tooth and ceramic wear: in vivo study.* Int J Prosthodont, 2008. **21**(3): p. 245-52.

16. Jacobi, R., H.T. Shillingburg, Jr., and M.G. Duncanson, Jr., *A comparison of the abrasiveness of six ceramic surfaces and gold.* J Prosthet Dent, 1991. **66**(3): p. 303-9.

17. Jagger, D.C. and A. Harrison, *An in vitro investigation into the wear effects of selected restorative materials on dentine.* J Oral Rehabil, 1995. **22**(5): p. 349-54.

18. DeLong, R., et al., *The wear of enamel when opposed by ceramic systems.* Dent Mater, 1989. **5**(4): p. 266-71.

19. Delong, R., M.R. Pintado, and W.H. Douglas, *The wear of enamel opposing shaded ceramic restorative materials: an in vitro study.* J Prosthet Dent, 1992. **68**(1): p. 42-8.

20. Hudson, J.D., G.R. Goldstein, and M. Georgescu, *Enamel wear caused by three different restorative materials.* J Prosthet Dent, 1995. **74**(6): p. 647-54.

21. Monasky, G.E. and D.F. Taylor, *Studies on the wear of porcelain, enamel, and gold.* J Prosthet Dent, 1971. **25**(3): p. 299-306.

22. Mahalick, J.A., F.J. Knap, and E.J. Weiter, *Occusal wear in prosthodontics.* J Am Dent Assoc, 1971. **82**(1): p. 154-9.

23. Archard, J., *Contact and rubbing of flat surfaces.* J Appl Phys, 1953. **24**: p. 981-988.

24. Attin, T., et al., *Correlation of microhardness and wear in differently eroded bovine dental enamel.* Arch Oral Biol, 1997. **42**(3): p. 243-50.

25. Oh, W.S., R. Delong, and K.J. Anusavice, *Factors affecting enamel and ceramic wear: a literature review.* J Prosthet Dent, 2002. **87**(4): p. 451-9.

26. William J. Callister, J., *Materials Science and Engineering An Introduction*. 2007, York, PA: John Wiley and Sons. 721.

27. DeLong, R., et al., *The wear of dental porcelain in an artificial mouth.* Dent Mater, 1986. **2**(5): p. 214-9.

28. Dahl, B.L. and G. Oilo, *In vivo wear ranking of some restorative materials.* Quintessence Int, 1994. **25**(8): p. 561-5.

29. Seghi, R.R., S.F. Rosenstiel, and P. Bauer, *Abrasion of human enamel by different dental ceramics in vitro.* J Dent Res, 1991. **70**(3): p. 221-5.

30. Oh, W.S., N.Z. Zhang, and K.J. Anusavice, *Effect of heat treatment on fracture toughness K(IC) and microstructure of a fluorcanasite-based glass-ceramic.* J Prosthodont, 2007. **16**(6): p. 439-44.

31. Mecholsky, J.J., Jr., *Fracture mechanics principles.* Dent Mater, 1995. **11**(2): p. 111-2.

32. Mecholsky, J.J., Jr., *Fractography: determining the sites of fracture initiation.* Dent Mater, 1995. **11**(2): p. 113-6.

33. Ekfeldt, A. and G. Oilo, *Occlusal contact wear of prosthodontic materials. An in vivo study.* Acta Odontol Scand, 1988. **46**(3): p. 159-69.

34. al-Hiyasat, A.S., W.P. Saunders, and G.M. Smith, *Three-body wear associated with three ceramics and enamel.* J Prosthet Dent, 1999. **82**(4): p. 476-81.

35. Metzler, K.T., et al., *In vitro investigation of the wear of human enamel by dental porcelain.* J Prosthet Dent, 1999. **81**(3): p. 356-64.

36. Imai, Y., S. Suzuki, and S. Fukushima, *Enamel wear of modified porcelains.* Am J Dent, 2000. **13**(6): p. 315-23.

37. Magne, P., et al., *Wear of enamel and veneering ceramics after laboratory and chairside finishing procedures.* J Prosthet Dent, 1999. **82**(6): p. 669-79.

38. Chantikul P, Anstis, GR., Lawn, BR, Marshall, DB, *A critical evaluation of indentation techniques for measuring fracture toughness: II strength method.* J Am Ceram Soc 1981. **64**: p. 539-543.

39. Parsell, D., *The optimization of glass-ceramic heat treatment schedules*, in *Materials Science Engineering*. 1993, University of Florida: Gainesville. p. 75.

40. Cesar, P.F., et al., *Correlation between fracture toughness and leucite content in dental porcelains.* J Dent, 2005. **33**(9): p. 721-9.

41. Denry, I.L. and J.A. Holloway, *Microstructural and crystallographic surface changes after grinding zirconia-based dental ceramics.* J Biomed Mater Res B Appl Biomater, 2006. **76**(2): p. 440-8.

42. Schweiger M, F.S., Cramer von Clausbruch S, Holand W, Rheinberger V, *Microstructure and properties of a composite system for dental applications composed of glass-ceramics in the SiO2-LiO-ZrO2-P2O5 system and ZrO2-ceramic (TZP).* J Mater Sci, 1999. **43**: p. 4563-4572.

43. Friel, J.J., *Practical Guide to Image Analysis*. 2000, Materials Park, OH: ASM International. 290.

44. Standard, E.-A. *Standard Test Methods for Determining Average Grain Size*. in *ASTM International*. 2004. West Conshohocken, PA.

45. Kaplan, D.B.a.W., *Microstructural Characterization of Materials*. second ed. 2008, West Sussex, PO19 8SQ, England: John Wiley and Sons Ltd.

46. Albakry, M., M. Guazzato, and M.V. Swain, *Influence of hot pressing on the microstructure and fracture toughness of two pressable dental glass-ceramics.* J Biomed Mater Res B Appl Biomater, 2004. **71**(1): p. 99-107.

47. Albakry, M., M. Guazzato, and M.V. Swain, *Biaxial flexural strength and microstructure changes of two recycled pressable glass ceramics.* J Prosthodont, 2004. **13**(3): p. 141-9.

48. Standard, E.-A., *Standard Test Method for Determining Volume Fraction by Systematic Manual Point Count*. 2008, ASTM International: West Conshohocken, PA 2008.

49. Say EC, C.A., Nobecourt A, Ersoy M, Guleryuz C, - *Wear and microhardness of different resin composite materials.* (- 0361-7734 (Print)).

50. Denry, I.L. and J.A. Holloway, *Effect of crystallization heat treatment on the microstructure and biaxial strength of fluorrichterite glass-ceramics.* J Biomed Mater Res B Appl Biomater, 2007. **80**(2): p. 454-9.

51. Hefter J, H.A., Mahoney ME, Harris JE, *Microstructural characterization of structural ceramics using image processing and analysis* J Am Ceram Soc, 1993. **76**(6): p. 1551-1557.

52. Chinn, R., *Grain sizes of ceramics by automatic image analysis.* J Am Ceram Soc, 1994. **77**(2): p. 589-592.

53. Thomas Hche, C.M., Issak Avramov, Christian Rssel, Wolfgang Heerrdegen, *Microstructure of SiO-AlO-CaO-PO-KO-F Glass Ceramics. 1. Needlelike versus isometric morphology of apatite crystals.* Chem Mater, 2001. **13**(4): p. 1312-1319.

54. Holand, W., et al., *A comparison of the microstructure and properties of the IPS Empress 2 and the IPS Empress glass-ceramics.* J Biomed Mater Res, 2000. **53**(4): p. 297-303.

55. Chung, K.H., et al., *The effects of repeated heat-pressing on properties of pressable glass-ceramics.* J Oral Rehabil, 2008.

56. Oh, S.C., et al., *Strength and microstructure of IPS Empress 2 glass-ceramic after different treatments.* Int J Prosthodont, 2000. **13**(6): p. 468-72.

57. Cattell, M.J., et al., *Flexural strength optimisation of a leucite reinforced glass ceramic.* Dent Mater, 2001. **17**(1): p. 21-33.

58. Lambrechts, P., Braem, M., Vuylsteke-Wauters, M., Vanherle, G., *Quantitative in vivo wear of human enamel.* J Dent Res 1989 **68**: p. 1752-1754.

59. Satish Chandra, S.C., Sourabh Chandra, *Textbook of Dental and Oral Anatomy Physilogy and Occlusion*. 2007, Noida: Gopsons Papers Ltd.

60. Holand, W., et al., *Needle-like apatite-leucite glass-ceramic as a base material for the veneering of metal restorations in dentistry.* J Mater Sci Mater Med, 2000. **11**(1): p. 11-7.

61. Holand, W.a.B.G., *Glass-Ceramic Technology*. 2002, Westerville, OH: The American Ceramic Society. 372.

62. Szabo I, N.B., Volksch G, Holand W, *Structure, chemical durability and microhardness of glass-ceramics containing apatite and leucite cyrstals.* Journl of Non-Crystalline Solids 2000. **272**: p. 191-199.

63. Guazzato, M., et al., *Strength, fracture toughness and microstructure of a selection of all-ceramic materials. Part I. Pressable and alumina glass-infiltrated ceramics.* Dent Mater, 2004. **20**(5): p. 441-8.

64. Guess, P.C., C.F. Stappert, and J.R. Strub, *[Preliminary clinical results of a prospective study of IPS e.max Press- and Cerec ProCAD- partial coverage crowns].* Schweiz Monatsschr Zahnmed, 2006. **116**(5): p. 493-500.

BIOGRAPHICAL SKETCH

Josephine Esquivel-Upshaw, D.M.D., M.S. is an associate professor in the Department of Prosthodontics at the University of Florida College of Dentistry. Dr. Esquivel received her D.M.D. degree from the University of the Philippines in 1991. She went on to specialize in the area of prosthodontics at Northwestern University Dental School in Chicago, IL, and completed her residency program and her master's degree in 1994. She came to the University of Florida as a clinical fellow in the Department of Prosthodontics in 1994 and became an assistant professor in 1995. After being promoted and tenured in 2001 to Associate Professor, Dr. Esquivel moved to the University of Texas Health Science Center at San Antonio in San Antonio, TX, to teach in the general dentistry department. She returned to the University of Florida in 2006. Her research focuses on ceramics and prosthesis survival for which she received K23 funding in May 2008, and a master's degree in medical sciences with a concentration in clinical and translational science in May 2010.